Atmos. Chem. Phys., 11, 13305–13323, 2011
www.atmos-chem-phys.net/11/13305/2011/
doi:10.5194/acp-11-13305-2011

Atmospheric Chemistry and Physics

Formation of semivolatile inorganic aerosols in the Mexico City Metropolitan Area during the MILAGRO campaign

V. A. Karydis[1,2], A. P. Tsimpidi[1,2], W. Lei[4], L. T. Molina[3,4], and S. N. Pandis[1,2,5]

[1]Institute of Chemical Engineering and High Temperature Chemical Processes, Foundation for Research and Technology Hellas, Patras, Greece
[2]Dept. of Chemical Engineering, University of Patras, Patras, Greece
[3]Dept. of Earth, Atmospheric and Planetary Sciences, Massachusetts Institute of Technology, USA
[4]Molina Center for Energy and the Environment (MCE2), La Jolla, CA 92037, USA
[5]Department of Chemical Engineering, Carnegie Mellon University, Pittsburgh, PA 15213, USA

Received: 10 June 2011 – Published in Atmos. Chem. Phys. Discuss.: 4 August 2011
Revised: 6 December 2011 – Accepted: 11 December 2011 – Published: 22 December 2011

Abstract. One of the most challenging tasks for chemical transport models (CTMs) is the prediction of the formation and partitioning of the major semi-volatile inorganic aerosol components (nitrate, chloride, ammonium) between the gas and particulate phases. In this work the PMCAMx-2008 CTM, which includes the recently developed aerosol thermodynamic model ISORROPIA-II, is applied in the Mexico City Metropolitan Area in order to simulate the formation of the major inorganic aerosol components. The main sources of SO_2 (such as the Miguel Hidalgo Refinery and the Francisco Perez Rios Power Plant) in the Mexico City Metropolitan Area (MCMA) are located in Tula, resulting in high predicted PM_1 (particulate matter with diameter less than 1 μm) sulfate concentrations (over 25 $\mu g\,m^{-3}$) in that area. The average predicted PM_1 nitrate concentrations are up to 3 $\mu g\,m^{-3}$ (with maxima up to 11 $\mu g\,m^{-3}$) in and around the urban center, mostly produced from local photochemistry. The presence of calcium coming from the Tolteca area (7 $\mu g\,m^{-3}$) as well as the rest of the mineral cations (1 $\mu g\,m^{-3}$ potassium, 1 $\mu g\,m^{-3}$ magnesium, 2 $\mu g\,m^{-3}$ sodium, and 3 $\mu g\,m^{-3}$ calcium) from the Texcoco Lake resulted in the formation of a significant amount of aerosol nitrate in the coarse mode with concentrations up to 3 $\mu g\,m^{-3}$ over these areas. PM_{1-10} (particulate matter with diameter between 1 and 10 μm) chloride is also high and its concentration exceeds 2 $\mu g\,m^{-3}$ in Texcoco Lake. PM_1 ammonium concentrations peak at the center of Mexico City (2 $\mu g\,m^{-3}$) and the Tula vicinity (2.5 $\mu g\,m^{-3}$). The performance of the model for the major inorganic PM components (sulfate, ammonium, nitrate, chloride, sodium, calcium, and magnesium) is encouraging. At the T0 measurement site, located in the Mexico City urban center, the average measured values of PM_1 sulfate, nitrate, ammonium, and chloride are 3.5 $\mu g\,m^{-3}$, 3.5 $\mu g\,m^{-3}$, 2.1 $\mu g\,m^{-3}$, and 0.36 $\mu g\,m^{-3}$, respectively. The corresponding predicted values are 3.7 $\mu g\,m^{-3}$, 2.7 $\mu g\,m^{-3}$, 1.7 $\mu g\,m^{-3}$, and 0.25 $\mu g\,m^{-3}$. High sulfate concentrations are associated with the transport of sulfate from the Tula vicinity, while in periods where southerly winds are dominant; the concentrations of sulfate are low. The underprediction of nitrate can be attributed to the underestimation of OH levels by the model during the early morning. Ammonium is sensitive to the predicted sulfate concentrations and the nitrate levels. The performance of the model is also evaluated against measurements taken from a suburban background site (T1) located north of Mexico City. The average predicted $PM_{2.5}$ (particulate matter with diameter less than 2.5 μm) sulfate, nitrate, ammonium, chloride, sodium, calcium, and magnesium are 3.3, 3.2, 1.4, 0.5, 0.3, 1.2, and 0.15 $\mu g\,m^{-3}$, respectively. The corresponding measured concentrations are 3.7, 2.9, 1.5, 0.3, 0.4, 0.6, and 0.15 $\mu g\,m^{-3}$. The overprediction of calcium indicates a possible overestimation of its emissions and affects the partitioning of nitric acid to the aerosol phase resulting occasionally in an overprediction of nitrate. Additional improvements are possible by improving the performance of the model regarding the oxidant levels, and revising the emissions and the chemical composition of the fugitive dust. The hybrid approach in which the mass transfer to the

Correspondence to: S. N. Pandis
(spyros@chemeng.upatras.gr)

Published by Copernicus Publications on behalf of the European Geosciences Union.

fine aerosol is simulated using the bulk equilibrium assumption and to the remaining aerosol sections using a dynamic approach, is needed in order to accurately simulate the size distribution of the inorganic aerosols. The bulk equilibrium approach fails to reproduce the observed coarse nitrate and overpredicts the fine nitrate. Sensitivity tests indicate that sulfate concentration in Tula decreases by up to 0.5 $\mu g\,m^{-3}$ after a 50 % reduction of SO_2 emissions while it can increase by up to 0.3 $\mu g\,m^{-3}$ when NO_x emissions are reduced by 50 %. Nitrate concentration decreases by up to 1 $\mu g\,m^{-3}$ after the 50 % reduction of NO_x or NH_3 emissions. Ammonium concentration decreases by up to 1 $\mu g\,m^{-3}$, 0.3 $\mu g\,m^{-3}$, and 0.1 $\mu g\,m^{-3}$ after the 50 % reduction of NH_3, NO_x, and SO_2 emissions, respectively.

1 Introduction

The rapid growth of megacities has led to serious urban air pollution problems in many developing countries. For example, Mexico City is the largest metropolitan area in North America with a population of 20 million. This megacity is experiencing high aerosol pollutant concentrations from a combination of high anthropogenic emissions, weak winds and intense sunshine (Molina and Molina, 2002). A large part of the $PM_{2.5}$ mass ($\sim$55 %) is inorganic, with sulfates, nitrates, ammonium, sodium and chloride being the dominant species. Nitrate can be found in both fine (particles with diameters less than 1 µm) and coarse (particles with diameters more than 1 µm) modes. The major source of NO_x, the gas phase precursor of nitrate, is mobile emissions from Mexico City. Sodium, chloride and the crustal components are mainly found in the coarse mode. The CEMEX cement plant in Tolteca, north of Mexico City, is a major source of calcium rich dust. Ammonium and sulfate are usually in the fine mode (Seinfeld and Pandis, 2006). The Miguel Hidalgo Refinery and the Francisco Perez Rios Power Plant in Tula are the major sources of SO_2 close to the MCMA. Mineral dust also plays an important role in the Mexico City atmosphere. Analysis of model and observational data in the Mexico City area during the MILAGRO (Megacity Initiative: Local and Global Research Observations) field experiment suggests that the large area of coastal dry lands to the northeast of Mexico City is an important source of dust particles for the entire MCMA. During dust aerosol events, observed from March 16 to 20 of 2006, dust aerosol mass accounts for about 70 % of the total PM_{10} (particulate matter with diameter less than 10 µm) aerosol mass concentrations, with a strong diurnal variation (Ying et al., 2011). These results also suggest that dust aerosols have important effects on actinic fluxes and therefore photochemistry in the MCMA.

The MILAGRO (http://www.eol.ucar.edu/projects/milagro/) field campaign was designed to follow the urban plume originating in Mexico City in order to study the evolution of the properties of trace gases and aerosols as they drifted downwind from a megacity. The study was conducted over multiple scales, ranging from ground-based investigations centered in the Mexico City metropolitan area to aircraft sampling over distances of hundreds of kilometres (Molina et al., 2010). The Intercontinental Chemical Transport Experiment-B (INTEX-B; Singh et al., 2009) was a major NASA-led multi-partner atmospheric field campaign (http://cloud1.arc.nasa.gov/intex-b/) operated as part of the MILAGRO campaign with a focus on observations over Mexico and the Gulf of Mexico. During MILAGRO/INTEX-B the extent and persistence of the outflow of pollution from Mexico were investigated (DeCarlo et al., 2008; Shinozuka et al., 2009; Voss et al., 2010). Several modeling studies combined with airborne measurements have focused on the evolution of the Mexico City plume (Arellano et al., 2007; Tie et al., 2009; Adhikary et al., 2010; Apel et al., 2010). A major component of the MILAGRO campaign was the use of the observed data to evaluate the performance of three dimensional chemical transport models and then use them for the design of emission control strategies.

Several atmospheric models have been developed based on thermodynamic equilibrium principles to predict inorganic atmospheric aerosol behavior. These include: EQUIL (Bassett and Seinfeld, 1983), MARS (Saxena et al., 1986), SEQUILIB (Pilinis and Seinfeld, 1987), AIM (Wexler and Seinfeld, 1991), SCAPE (Kim et al., 1993b, a), SCAPE2 (Kim and Seinfeld, 1995; Meng et al., 1995), EQUISOLV (Jacobson et al., 1996), AIM2 (Clegg et al., 1998b, a), ISORROPIA (Nenes et al., 1998), GFEMN (Ansari and Pandis, 1999a) and EQUISOLV II (Jacobson, 1999). In thermodynamic models, the gas and aerosol phases are assumed to be always in equilibrium assuming that mass transfer is much faster than the time-step of the model. The advantage of these models is their speed, simplicity, and stability. Nevertheless, for particles much larger than approximately 1 µm, the assumption of thermodynamic equilibrium introduces substantial error, since their equilibrium timescale can be an hour or longer (Meng and Seinfeld, 1996; Dassios and Pandis, 1999). On the other hand, dynamic models, continuously simulate the mass transfer between each particle group and the gas phase. Examples of such models are MOSAIC (Zaveri et al., 2008), MADM (Pilinis et al., 2000), UCD (Zhang and Wexler, 2008). Although these models are the most accurate, they are much more computationally intensive than the thermodynamic equilibrium models. Equilibrium models have been used in determining emissions control strategies (Watson et al., 1994; Ansari and Pandis, 1998; Kumar et al., 1998), in analyzing ambient measurements (Ansari and Pandis, 1999b, 2000) and directly in large-scale chemical transport models (Pilinis and Seinfeld, 1988; Lurmann et al., 1997; Jacobson et al., 1996; Jacobson, 1997a, b; Meng et al., 1998; Nenes et al., 1999). Several studies have been performed comparing field measurements of inorganic gaseous species and their

particulate forms versus theory (Tanner, 1982; Hildemann et al., 1984). Tanner (1982) compared theoretical equilibrium calculations versus observed partial pressure products of nitric acid and ammonia for Long Island, NY and reported a general agreement during daytime. Nevertheless, during nighttime, the predicted ammonia concentrations were much lower and the nitric acid concentrations much higher than the observed values. Hildemann et al. (1984) performed a similar comparison between equilibrium-based calculations and observed partial pressure products of nitric acid and ammonia and their particulate forms at different locations in Southern California. At inland sites like Anaheim and Rubidoux, particulate and gaseous pollutant concentrations were readily explained if the aerosol was assumed to exist as an external mixture with all particulate nitrate and ammonium available to form pure NH_4NO_3. At monitoring sites near the coast, like Long Beach, aerosol nitrate was found in the presence of NH_3 and HNO_3 concentrations that thermodynamic calculations showed are too low to produce pure NH_4NO_3. Although comparison of calculated and observed partial pressure products of NH_3 and HNO_3 can provide an alternative way of testing an atmospheric equilibrium model, interpretations of these comparisons are often difficult, especially in evaluating the ability of these models to reproduce particulate nitrate concentrations. An analysis of model performance against particulate matter measurements has been performed among others by Russell et al. (1988), Pilinis and Seinfeld (1987), Wexler and Seinfeld (1991), Kumar et al. (1998), Ansari and Pandis (1999b), and Zhang et al. (2000, 2002). The first multicomponent particulate matter atmospheric models were developed and applied in California. An Eulerian model was used to describe the transport and formation of pollutants in the south California air basin by Russell et al. (1988). A three-dimensional Eulerian CTM simulating the major inorganic and organic PM components and their size distribution was developed by Pilinis and Seinfeld (1987). Both of these initial models were evaluated in Los Angeles for the 30–31 August 1982 smog episode. Wexler and Seinfeld (1991) developed a model of the temporal composition of atmospheric aerosol particles based on their transport and thermodynamic properties. Components of the model were tested against measurements of activity coefficients in single- and multi-component aqueous solutions and general agreement was found. Kumar et al. (1998) compared the performance of several equilibrium models against measurements taken during the 1995 Integrated Monitoring Study (Chow and Egami, 1997). In these cases, the mean predictions of PM_{10} nitrate and ammonium agreed within 20–30 % of the corresponding measurements. Ansari and Pandis (1999b) compared the performance of SEQUILIB, SCAPE2, ISORROPIA and GFEMN and found a general agreement in predictions for particulate nitrate and total inorganic particulate matter (PM) over a broad range of temperature, relative humidity (RH) and composition. However, they found significant differences in predictions for particulate water concentrations as the first three do not adequately reproduce multistage deliquescence behavior for multi-component systems. Against measurements from the Southern California Air Quality Study (SCAQS, Lawson, 1990), all models qualitatively reproduced but generally underpredicted $PM_{2.5}$ nitrate concentrations (mean normalized biases less than 30 %). Zhang et al. (2000) compared the performance of SCAPE2, AIM2, MARS-A, SEQUILIB, and EQUISOLV II and found that although the PM compositions and concentrations predicted by these modules were generally comparable under a broad range of RH and composition, significant discrepancies existed under some conditions, especially at high nitrate/chloride concentrations and low/medium RHs. As a consequence, the absolute differences in total PM concentrations predicted by these modules under all simulation conditions were 7.7–12.3 % on average and as much as 68 % for specific cases. Data obtained during the 1999 Atlanta Supersite Experiment was used to test the validity of the assumption of thermodynamic equilibrium between the inorganic fine particulate matters and their gas-phase phase precursors (Zhang et al., 2002). The equilibrium gas-phase concentrations were calculated using the ISORROPIA model which was predicting the equilibrium NH_3(g) generally less than its observed concentration and the HNO_3(g) generally greater than the observed concentration.

Several photochemical modeling studies have been carried out in the MCMA. Among them, Zhang et al. (2009) and Tie et al. (2009) used the fully coupled WRF/CHEM (Weather Research and Forecasting – Chemistry) model to study the origin and evolution of the gaseous criteria pollutants (CO, O_3, NO_x, NO_y) during the MILAGRO and MIRAGE-Mex field campaigns, respectively. Song et al. (2010) investigated the response of ozone formation to anthropogenic emission changes using CAMx driven by WRF meteorology. However, there have been rather limited efforts to predict particle concentrations in Mexico City by using three-dimensional CTMs. Tsimpidi et al. (2010, 2011) applied PMCAMx-2008 simulating the organic aerosol formation during the MCMA-2003 and MILAGRO-2006 campaigns by using the volatility basis set framework assuming that both primary and secondary organic components are semi-volatile and photochemically reactive. Hodzic et al. (2009, 2010) used CHIMERE to study the contribution of biogenic organic compounds and semivolatile primary organic compounds to the formation of secondary organic aerosols in Mexico City during the MILAGRO field project. Li et al. (2011a), Shrivastava et al. (2011), and Fast et al. (2009) simulated the organic aerosol concentrations in Mexico City using the WRF/CHEM model. Li et al. (2011b) further evaluated the impact of aerosol on photochemistry in Mexico City using WRF/CHEM during MILAGRO. Even fewer studies have focused on the formation of the inorganic aerosols in Mexico City. Fountoukis et al. (2009) coupled fast measurements of aerosol and gas-phase constituents with the

ISORROPIA-II thermodynamic model to study the partitioning of semivolatile inorganic species and phase state of Mexico City aerosol during the MILAGRO 2006 campaign. Karydis et al. (2010) introduced the ISORROPIA-II model into PMCAMx-2008 and applied it to the MCMA in order to simulate the chemical composition and mass of the major PM_1 (fine) and PM_{1-10} (coarse) inorganic components and determine the effect of mineral dust on their formation during a week of April 2003. However, major sources which are located approximately 100 km north-northwest of Mexico City center (in the Tula industrial area) were not included in the model domain resulting in a small underprediction of all semivolatile inorganic components. The Karydis et al. (2010) study was also limited by the availability of measurements in Mexico City and the surrounding area (there was just one site with continuous PM composition measurements).

The present study adds to these previous efforts evaluating our current understanding of the atmospheric processes responsible for the spatial and temporal variability of fine inorganic PM over the Mexico City Metropolitan Area. The organic aerosol sources, concentrations and processes have been discussed in our recent paper (Tsimpidi et al., 2011). Briefly, the average PM_1 OA has been predicted to be equal to $18\,\mu g\,m^{-3}$ (versus $17.2\,\mu g\,m^{-3}$ measured) and $11.6\,\mu g\,m^{-3}$ (versus $11\,\mu g\,m^{-3}$ measured) at T0 and T1 respectively. This study will focus exclusively on the inorganic PM components. In particular, the new thermodynamic model ISORROPIA-II, in which the thermodynamics of the crustal elements of calcium, potassium and magnesium have been added to the preexisting suite of components of the ISORROPIA model, has been incorporated in the three dimensional chemical transport model PMCAMx. The new model combines the computational advantages of ISORROPIA with the explicit treatment of thermodynamics of crustal species. Size-resolved composition of particles is simulated using the hybrid method for aerosol dynamics, in which the mass transfer to the fine aerosol sections (up to 1 µm) is simulated using the bulk equilibrium assumption and to the remaining aerosol sections using the dynamic approach and MADM. The model domain is expanded, compared to Karydis et al. (2010) study focusing on the MCMA-2003 campaign in the same area, in order to include major sources from refineries and industries, a more accurate chemical composition of the fugitive dust emissions is used, and the model predictions are evaluated against measurements from two sites; one in the urban area of Mexico City, designated as T0 and located in Northeast Mexico City at the Instituto Mexicano del Petroleo (IMP), and T1, located at a suburban location approximately 32 km north of IMP (Querol et al., 2008). The evaluation focuses on the ability of PMCAMx-2008 to reproduce not only daily average concentrations but also the diurnal variation of the major inorganic aerosol components during March 2006.

2 Model description

PMCAMx-2008 uses the framework of CAMx (Environ, 2003), which models the processes of horizontal and vertical advection, horizontal and vertical dispersion, wet and dry deposition, and gas-phase chemistry. In addition, three detailed aerosol modules are used: inorganic aerosol growth (Gaydos et al., 2003; Koo et al., 2003), aqueous-phase chemistry (Fahey and Pandis, 2001), and secondary organic aerosol formation and growth (Lane et al., 2008). PMCAMx-2008 is the research version of the publicly available CAMx model.

The aerosol species treated are sulfate, nitrate, ammonium, chloride, potassium, calcium, magnesium, elemental carbon, and primary and secondary organics. The aerosol size and composition distribution is simulated using a sectional representation across 10 size bins with the wet diameter varying from 40 nm to 40 µm. The chemical mechanism used is based on the SAPRC99 mechanism (Carter, 2000; Environ, 2003) which contains 211 reactions with 56 gases and 18 radicals.

The amount of each inorganic species transferred between the gas and aerosol phases is determined by using the hybrid approach (Capaldo et al., 2000) for aerosol thermodynamics along with ISORROPIA II (Fountoukis and Nenes, 2007) which is a computationally efficient code that treats the thermodynamics of K^+-Ca^{2+}-Mg^{2+}-NH_4^+-Na^+-SO_4^{2-}-NO_3^--Cl^--H_2O aerosol systems. According to the hybrid method, the aerosol particles with diameters less than the threshold diameter (1 µm for the purposes of this study) are simulated assuming equilibrium while for the particles larger than the threshold diameter the improved MADM model of Pilinis et al. (2000), as extended by Gaydos et al. (2003), is used, which ensures a stable solution, regardless if the particles are completely dry, with an aqueous phase or transition between acidic and neutral conditions. Equilibrium is assumed between the gas and organic aerosol phase based on the Volatility Basis Set approach, VBS (Lane et al., 2008; Murphy and Pandis, 2009). The aerosol mass is distributed over the aerosol size distribution by using a weighting factor for each size section based on the effective surface area (condensational sink) of each size section (Pandis et al., 1993; Lurmann et al., 1997).

3 Model application

PMCAMx-2008 is used to simulate air quality in the MCMA during March of 2006. The first three days of each simulation have been excluded in order to limit the effect the initial conditions have on the results. The concentrations of the aerosol components at the boundaries of the domain were chosen based on results of the GISS-II' global CTM (Racherla and Adams, 2006). The GISS-II results generated a climatological background of aerosols in the area around the PMCAMx model domain with the aerosol values representing a 5-year

Table 1. Aerosol concentrations ($\mu g\,m^{-3}$) at the boundaries of the domain.

Species	South Boundary	West Boundary	East Boundary	North Boundary
Sulfate	1.7	3.0	2.6	1.4
Ammonium	0.3	1.0	1.0	0.4
Nitrate	1.4	0.7	1.2	1.2
Chloride	3.2	0.8	1.1	1.1
Sodium	2.7	0.7	1	0.9
Calcium	0.1	0.1	0.1	0.1
Magnesium	0.2	0.1	0.1	0.1
Potassium	0.1	0.1	0.1	0.1
Organic Mass	7.0	8.0	11.5	5.0

average for the month of March (Table 1). The boundary conditions (BCs) are assumed to be invariant with height and along each boundary. In order to estimate the effect the BCs have on the predicted inorganic aerosol concentrations, a sensitivity simulation has been conducted where the only source of aerosols is the BCs (zero emissions). Based on the results of the base case and the BC-sensitivity case simulation, at T0, the percentage of the predicted PM_{10} sulfate, total (gas and aerosol) nitrate, total ammonium, total chloride, sodium, calcium, potassium, and magnesium that is coming from the BCs is 37, 12, 3, 38, 45, 6, 27, and 26 %, respectively. This fraction is, as expected, high close to the boundaries and very small close to sources such as Tula vicinity for sulfate (4 %) and ammonium (11 %), Mexico City center for nitrate (9 %) and ammonium (3 %), Tolteca vicinity for nitrate (9 %) and calcium (1 %), and Texcoco Lake for chloride (25 %), sodium (28 %), potassium (6 %), and magnesium (5 %). Based on these results, BCs (for species other than sodium chlroride) have a small impact close to sources and thus they do not affect the conclusions of this study. Sodium and chloride are significantly influenced from the imposed south BCs. These are the upper limits of the effects of the BCs in the upper layers of the model, as they include the effects of all the layers.

The modeling domain covers a 210×210 km region centered in the MCMA with 3×3 km grid resolution and fifteen vertical layers extending to 6 km above ground level (Fig. 1). Inputs to the model include horizontal wind components, temperature, pressure, water vapor, vertical diffusivity, clouds, and rainfall, all computed offline by the Weather Research and Forecast (WRF) model (WRF v2.2.1; Michalakes et al., 2005). The maximum time step in the CTM is 10 min and the CTM output frequency is user-selected. The WRF simulation for March 2006 used three one-way nested grids with horizontal resolutions of 36, 12, and 3 km and 35 sigma levels in the vertical direction. The PMCAMx model subdomain was similar to the WRF D3 domain (same map projection, same domain center and same horizontal grid resolution). To improve the accuracy of the simulated fields, a

Fig. 1. The modeling domain for the Mexico City Metropolitan Area during the MILAGRO campaign. It also shows the locations of the monitoring stations during the campaign.

continuous four dimensional data assimilation scheme was employed in the domain with an horizontal resolution of 3 km. Multi-level upper-air observations were assimilated, including radar wind profilers, tethered balloon measurements, controlled meteorological balloon observations, aircraft observations, additional soundings inside the Mexico City basin operated during the MILAGRO campaign, and routine soundings observations. Details of the WRF setup are described by Song et al. (2010).

The emission inventory used is based on the MCMA 2006 official emission inventory (http://www.sma.df.gob.mx/sma/links/download/archivos/ie06_criterio_pw.pdf) and has been expanded to the modeling domain of this study in order to include major emission sources outside of the MCMA such as the refineries and the power plants located in the Tula vicinity (Table 2). Figure 2 depicts the spatial distribution of NO_x, NH_3, SO_2, and mineral dust emissions used in this study. The area emissions outside the MCMA were estimated based on the population distribution. Biogenic emissions were estimated using the WRF-driven MEGAN v2.04 model (Model of Emissions of Gases and Aerosols from Nature) developed by Guenther et al. (2006). The anthropogenic emissions were evaluated based on the comprehensive data from the field campaign and the routine ambient air quality monitoring network. Details of the anthropogenic emission estimation are described in Song et al. (2010). Volcanic emissions are also explicitly included in the emission inventory but biomass-burning emissions are not. The latter are introduced in the model through the boundary conditions based on the measurements and analysis of Crounse et

Table 2. Domain wide emissions (tons day^{-1}) of the inorganic aerosol precursors and components.

Species	NO_x	SO_2	NH_3	Cl^-	Na^+	K^+	Ca^+	Mg^+	Mineral Dust
Total Emissions	688	2831	110	15	96	106	318	69	6821

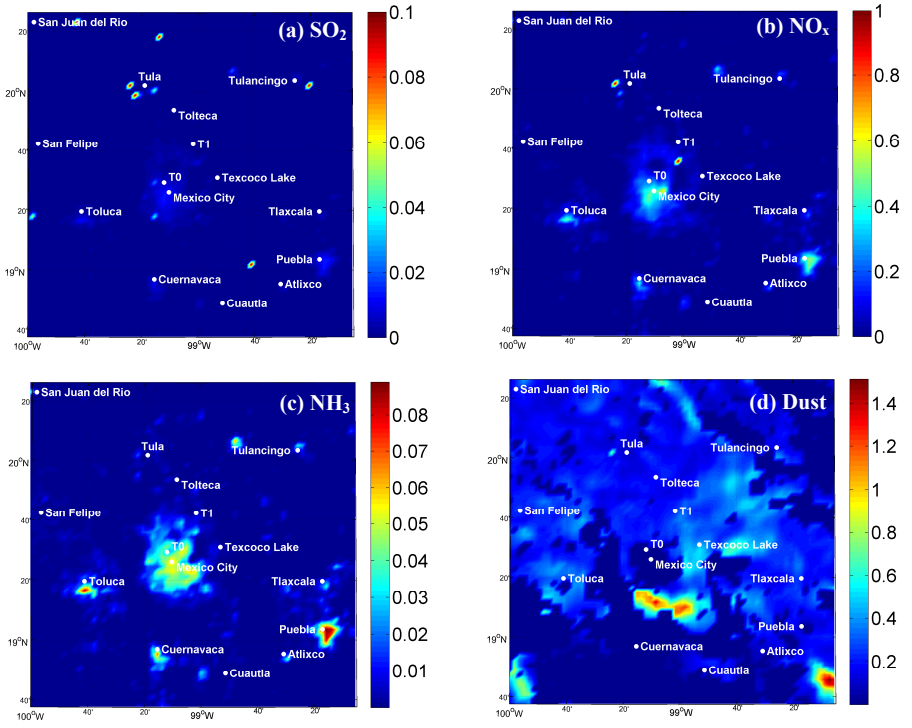

Fig. 2. Spatial distribution of total emissions of **(a)** SO_2, **(b)** NO_x, **(c)** NH_3, and **(d)** Dust (tons day^{-1} km^{-2}). SO_2 and NO_x emissions from Tula are up to 30 and 2.5 tons day^{-1} km^{-2}, respectively.

al. (2009) for the MILAGRO period. The emission inventory also includes improved dust and sodium chloride emissions, based on the approach of Karydis et al. (2010), as well as new HONO emissions (0.8 % of the NO_x emissions based on Aumont et al., 2003). The improved dust emissions are the only emissions which are different for each day of simulation and they were calculated based on the algorithm of Draxler et al. (2001), which uses the concept of a threshold friction velocity dependent on surface roughness. Emissions of individual dust species (sodium, potassium, calcium, magnesium) are estimated as a constant fraction of total dust emissions. This fraction is determined based on the geological materials that exist in the different regions of the model domain and produce fugitive dust emissions according to the findings of Vega et al. (2001). Fugitive dust sources in and around MCMA include unpaved and paved roads, agricultural soil, dried lake, asphalt, cement plants, landfill, gravel, and tezontle soil. The pollutant emissions are introduced in the model every hour during the simulation.

4 Overview of model predictions

The predicted average ground-level concentrations of PM_1 sulfate, nitrate, ammonium, and chloride over the period of March 2006 are shown in Fig. 3. The highest predicted sulfate concentrations are over the Tula vicinity (over 25 µg m^{-3}), coming from the large SO_2 sources from the industrial complexes in the area. In the center of Mexico City, there are no major SO_2 sources, and sulfate concentrations are lower (up to 5 µg m^{-3}). Nitrate is enhanced significantly in the urban area and immediate outflow (up to 3 µg m^{-3}), mostly produced from local photochemistry, indicating a strong urban source. Nitrate decreases with distance from the city, due to evaporation and deposition (of HNO_3 vapor), remaining in low levels in the surroundings (lower than 1 µg m^{-3}). Ammonium concentrations peak at the center of Mexico City (2 µg m^{-3}) and the Tula vicinity (2.5 µg m^{-3}) existing mainly in the form of ammonium nitrate and ammonium sulfate, respectively. Predicted PM_1 chloride concentrations are generally low (less than 0.5 µg m^{-3} in the entire

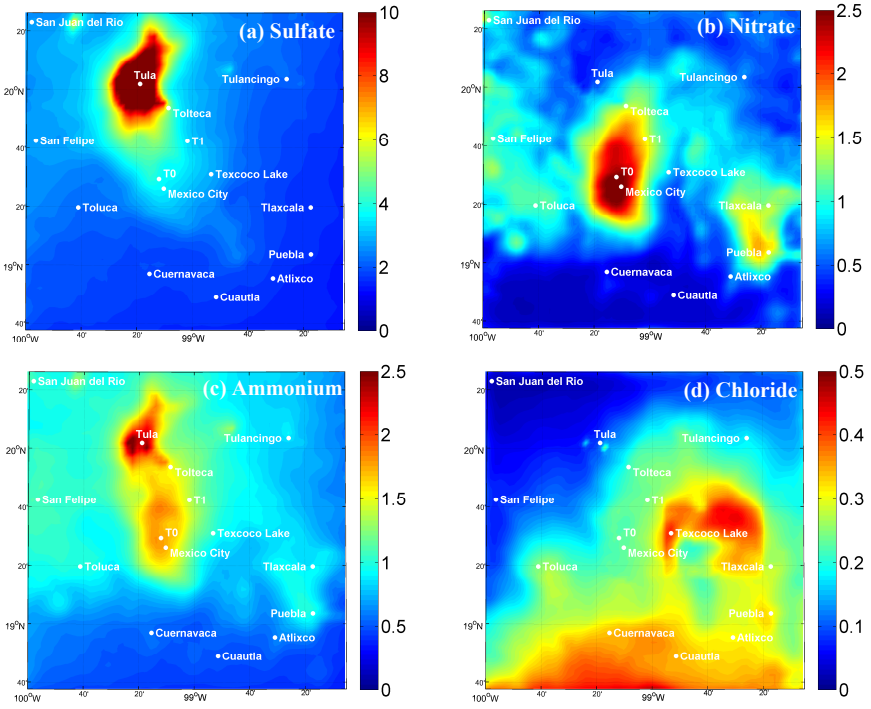

Fig. 3. Predicted average ground level concentrations of PM_1 **(a)** sulfate, **(b)** nitrate, **(c)** ammonium, and **(d)** chloride ($\mu g\,m^{-3}$) during 4–30 March 2006.

model domain) with the highest values in the Texcoco dry Lake and the south area of the domain, influenced by the high south boundary conditions.

The results for the coarse (PM_{1-10}) sulfate, nitrate, ammonium, chloride, sodium, calcium, potassium, and magnesium are shown in Fig. 4. The Texcoco dry Lake is a significant source of potassium ($1\,\mu g\,m^{-3}$), magnesium ($1\,\mu g\,m^{-3}$), sodium ($2\,\mu g\,m^{-3}$), and calcium ($3\,\mu g\,m^{-3}$). Coarse calcium concentrations peak around Tolteca ($7\,\mu g\,m^{-3}$), which is located around 70 km north of the Mexico City, due to the cement industries in the area. ISORROPIA II along with the hybrid approach assist in simulating the formation of PM_{1-10} nitrate and chloride describing interactions between these anions and the cations of mineral dust. The presence of calcium coming from the Tolteca vicinity as well as the rest of the mineral cations from the Texcoco Lake resulted in the formation of a significant amount of aerosol nitrate in the coarse mode with concentrations up to $3\,\mu g\,m^{-3}$. PM_{1-10} chloride is also high and its concentration exceeds $2\,\mu g\,m^{-3}$ in Texcoco Lake. There is also a little ammonium in the coarse mode (less than $0.5\,\mu g\,m^{-3}$), even if the coarse dust particles are alkaline. The soluble crustal elements increase the PM water content and thus favor the ammonium nitrate formation. Phase equilibrium between the gas and aerosol-phases (Seinfeld and Pandis, 2006) results in the equality between the water activity, α_w, and the ambient fractional relative humidity, RH (expressed on a 0.0 to 1.0 scale). The water content of aerosols is calculated using the ZSR relationship (Stokes and Robinson, 1966). The addition of the soluble crustal elements, especially magnesium, increases the water content in the coarse mode (under the same RH) which eventually shifts the reversible reaction of NH_3 with HNO_3 towards the aerosol phase producing more ammonium nitrate (Nguyen et al., 1997; Finlayson-Pitts and Pitts, 2000). Appreciable amounts of aerosol water (hence ammonium nitrate) is present even at moderate RH, given that some of the mineral salts deliquesce at low to moderate RH (e.g., 33 % for $MgCl_2$ and 54 % for $Mg(NO_3)_2$ at 298 K). In particular, the aerosol water content near Texcoco Lake and near the Tolteca cement plant increased by 45 and 35 % respectively after the addition of the crustal element thermodynamics in the model.

5 Model evaluation

The ability of PMCAMx and WRF-Chem to reproduce the observed concentrations of trace gases that affect inorganic aerosols during MILAGRO has been discussed in previous publications (Li et al., 2010; Song et al., 2010; Tsimpidi et al., 2011; Li et al., 2011a). These studies have used the same emissions and meteorological fields as the present study. Song et al. (2010) investigated the performance of the CTM CAMx under five different sets of meteorological conditions in the MCMA during the MILAGRO field campaign.

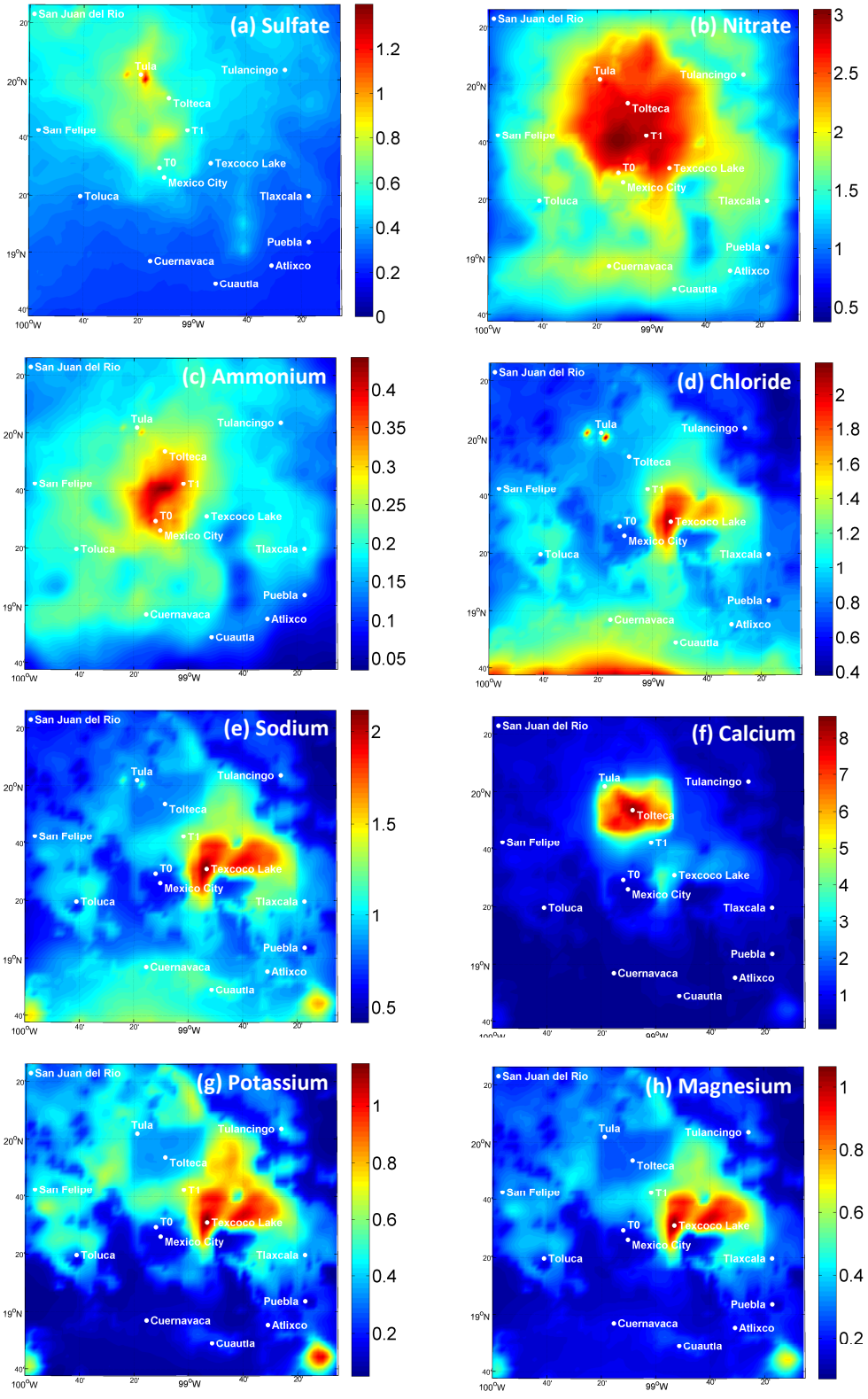

Fig. 4. Predicted average ground level concentrations of PM_{1-10} **(a)** sulfate, **(b)** nitrate, **(c)** ammonium, **(d)** chloride, **(e)** sodium, **(f)** calcium, **(g)** potassium, and **(h)** magnesium ($\mu g\, m^{-3}$) during 4–30 March 2006.

Table 3. Comparison of PMCAMx predictions with hourly observations taken at T0 during 10–31 March 2006.

PM_1 Species	Data Points	Mean Obs. ($\mu g\,m^{-3}$)	Mean Sim. ($\mu g\,m^{-3}$)	MB ($\mu g\,m^{-3}$)	MAGE ($\mu g\,m^{-3}$)	RMSE ($\mu g\,m^{-3}$)	NMB	NME
Sulfate	450	3.54	3.68	0.14	2.04	2.84	0.04	0.58
Nitrate	450	3.51	2.66	−0.85	2.15	3.29	−0.24	0.61
Ammonium	450	2.07	1.74	−0.33	1.03	1.42	−0.16	0.50
Chloride	450	0.36	0.25	−0.11	0.32	0.50	−0.32	0.89

Table 4. Comparison of PMCAMx predictions with hourly observations taken at T1 site during 10–31 March 2006.

PM_1 Species	Data Points	Mean Obs. ($\mu g\,m^{-3}$)	Mean Sim. ($\mu g\,m^{-3}$)	MB ($\mu g\,m^{-3}$)	MAGE ($\mu g\,m^{-3}$)	RMSE ($\mu g\,m^{-3}$)	NMB	NME
Sulfate	451	3.74	3.3	−0.44	1.87	2.82	−0.12	0.50
Nitrate	448	2.92	3.18	0.26	2.25	3.10	0.1	0.77
Ammonium	342	1.45	1.35	−0.10	1.07	1.43	0.07	0.74
Sodium	304	0.30	0.47	0.17	0.20	0.32	0.56	0.70
Chloride	278	0.44	0.28	−0.16	0.45	0.78	−0.36	1.02
Calcium	399	0.62	1.19	0.57	1.14	2.50	0.93	1.14
Magnesium	373	0.15	0.15	0.00	0.12	0.18	0.04	0.82

Simulated plume mixing and transport were examined through comparisons with airborne measurements. The observed concentrations of ozone precursors and ozone were reasonably well reproduced. Nevertheless, Tsimpidi et al. (2011) reported that OH levels are underestimated during early morning even though they are reasonably reproduced by the model (PMCAMx-2008) during the rest of the day. Li et al. (2010) identified HONO production and emissions as an important source of OH during the early morning.

Ground Observations: To evaluate the model results for the inorganic aerosol components within the city during March 2006 we used measurements of inorganic aerosols collected at two supersites, at the Instituto Mexicano del Petroleo (designed as T0) and at Universidad Tecnologica de Tecamac (designed as T1). The T0 monitoring station was located to the northwestern part of the basin of Mexico City. It is an urban background site influenced by road traffic emissions (300 m from four major roads surrounding it), domestic and residential emissions, but also potentially influenced by local industrial emissions and from the Tula industrial area (60 km to the north-northwest, in Hidalgo State). T1 was a suburban background site located around 50 km to the north of Mexico City, in an area isolated from major urban agglomerations but close to small populated agglomerations, and around 500 m from the closest road.

For T0 we used high-resolution time-of flight Aerosol Mass Spectrometer (ToF-AMS) (DeCarlo et al., 2006) measurements of PM_1 inorganic components (NH_4^+, SO_4^{2-}, NO_3^-, Cl^-) that are reported with more details by Aiken et al. (2009). For T1 we used $PM_{2.5}$ ion concentration observations of NH_4^+, SO_4^{2-}, NO_3^-, Na^+, Cl^-, Ca^{2+}, K^+, Mg^{2+} (Fountoukis et al., 2009; Moya et al., 2011) measured by a Particle Into Liquid Sampler (PILS) with a 6-min sampling period and a new chromatogram being started every 17 min (Orsini et al., 2003). The advantage of this instrument is the simultaneous measurements of important inorganic anions and cations at high time-resolution. A complete list with all the research groups that contributed to the measurements during the MILAGRO campaign can be found in Molina et al. (2010).

The results of the comparison between the model predictions and the measurements are depicted in Figs. 5–9. The mean bias (MB), mean absolute gross error (MAGE), normalized mean bias (NMB), normalized mean error (NME), and the root mean square error (RMSE) were also calculated (Tables 3, 4) to assess the model performance:

$$\mathrm{MAGE} = \frac{1}{N}\sum_{i=1}^{N}|\mathrm{P}_i - \mathrm{O}_i| \qquad \mathrm{MB} = \frac{1}{N}\sum_{i=1}^{N}(\mathrm{P}_i - \mathrm{O}_i)$$

$$\mathrm{NME} = \frac{\sum_{i=1}^{N}|\mathrm{P}_i - \mathrm{O}_i|}{\sum_{i=1}^{N}\mathrm{O}_i} \qquad \mathrm{NMB} = \frac{\sum_{i=1}^{N}(\mathrm{P}_i - \mathrm{O}_i)}{\sum_{i=1}^{N}\mathrm{O}_i}$$

$$\mathrm{RMSE} = \left[\frac{1}{N}\sum_{i=1}^{N}(\mathrm{P}_i - \mathrm{O}_i)^2\right]^{\frac{1}{2}}$$

where P_i is the predicted value of the pollutant concentration, O_i is the observed value of the concentration at the same time, and N is the total number of the measurements used for

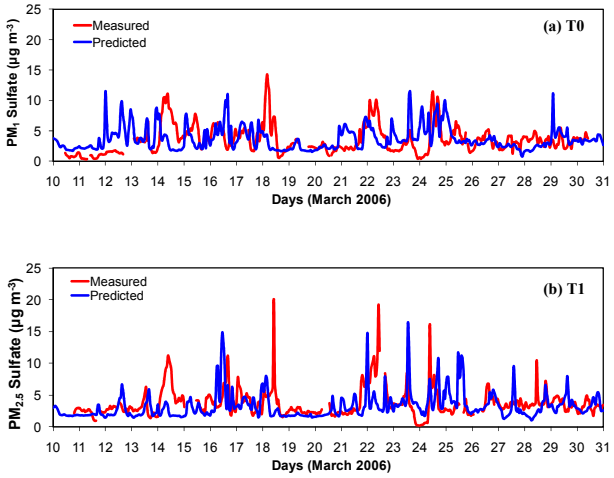

Fig. 5. Comparison of model hourly predictions against measurements for PM_1 sulfate taken at T0 **(a)** and $PM_{2.5}$ sulfate taken at T1 **(b)**, during the MILAGRO campaign.

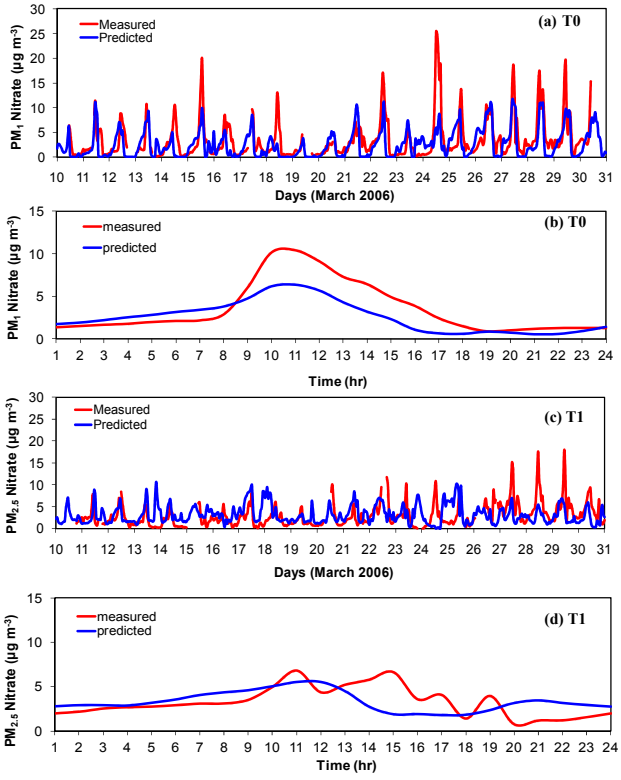

Fig. 6. Comparison of model hourly and diurnal predictions against measurements for PM_1 nitrate taken at T0 **(a, b)** and $PM_{2.5}$ nitrate taken at T1 **(c, d)** during the MILAGRO campaign.

the comparison. NME (in %) and MAGE (in $\mu g\,m^{-3}$) give an estimation of the overall discrepancy between predictions and observations, while NMB (in %) and MB (in $\mu g\,m^{-3}$) are sensitive to systematic errors. RMSE (in $\mu g\,m^{-3}$) incorporates both the variance of the prediction and its bias. The predicted and the measured values are compared for every single hour during the simulation period.

Sulfate: The performance of the model for sulfate is encouraging in both T0 and T1 sites (Fig. 5). Sulfate peaks at T1 and T0 sites are the result of transport of the high concentrations of sulfate produced near Tula. When the winds at T1 and T0 are northerly, high sulfate concentrations are observed (or predicted) in these sites, while in periods where southerly winds are dominant, the concentrations of sulfate are low. In T0 the average predicted PM_1 sulfate concentration is $3.7\,\mu g\,m^{-3}$ while the observed average was $3.5\,\mu g\,m^{-3}$. Both the model and the measurements show little variability in the average diurnal sulfate concentration profile. In T1 the measured $PM_{2.5}$ sulfate concentration was variable with concentration spikes up to $15\,\mu g\,m^{-3}$ as the location of this station is closer to the Tula vicinity which is the major source of sulfate. The model does reproduce this behavior even if some of the spikes are not at the right times. This discrepancy between the measured and the predicted profiles is partially due to the use of the same emission inventory for SO_2 for every day. Errors in the meteorology were also identified as a major cause of some of the discrepancies between model predictions and measurements. For instance, during 18 March the model underpredicts sulfate in both measurement sites (Fig. 5a, b). According to the measurements, the sulfate produced in Tula during the early morning of the 18th was transported to the southeast and appeared in T1 ($20\,\mu g\,m^{-3}$) and T0 ($15\,\mu g\,m^{-3}$) at around noon of the same day. On the other hand, WRF predicts a shift in wind direction from northerly to southerly several hours earlier than it should. As a result the model misses the observed sulfate concentration peak on that day in both T1 and T0 sites. The predicted average $PM_{2.5}$ sulfate concentration in T1 is $3.3\,\mu g\,m^{-3}$ while the measured average was $3.7\,\mu g\,m^{-3}$.

Nitrate: Both PMCAMx-2008 and measurements suggest that nitrate peaks during noon at T0 (Fig. 6a) and a couple of hours later at T1 with a lower concentration (Fig. 6c). During nighttime, predicted nitrate remains low (a few $\mu g\,m^{-3}$) in both sites, which is consistent with the measurements. During noon, there are several high nitrate concentration (above $10\,\mu g\,m^{-3}$) measurement periods in the dataset during which the model tends to underpredict the nitrate levels. Comparisons of the predicted and measured diurnal nitrate profiles at T0 (Fig. 6b) suggest that the model underpredicts nitrate during noon as the predicted formation of nitrate during the early morning hours is not as rapid as the observations. This discrepancy is not the result of errors in the partitioning of the available nitric acid (Fountoukis et al., 2007) but to an underprediction of the total nitric acid. In particular, the average value of the measured total nitric acid during its peak hour (at 11:00 LT) was 4.6 ppb (Aiken et al., 2009; Zheng et al., 2008) while the average predicted total nitrate at the

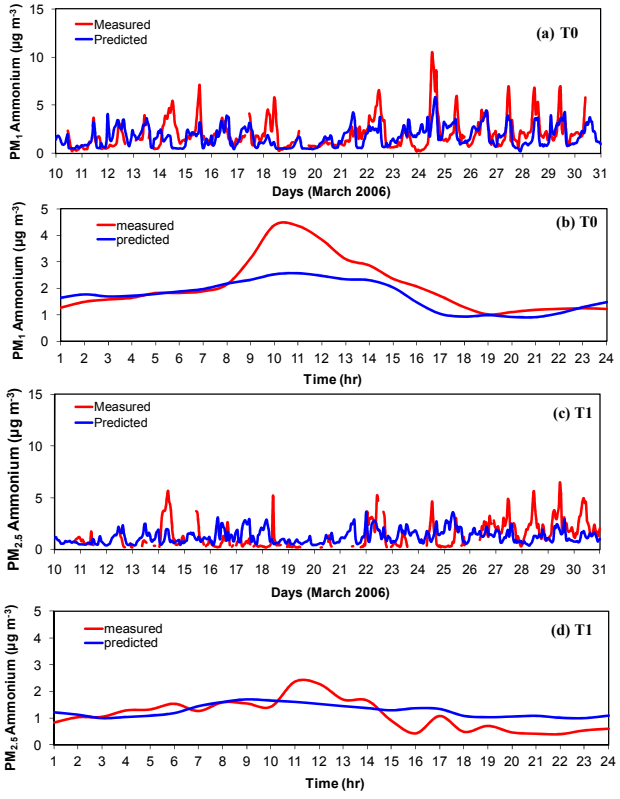

Fig. 7. Comparison of model hourly and diurnal predictions against measurements for PM_1 ammonium taken at T0 **(a, b)** and $PM_{2.5}$ ammonium taken at T1 **(c, d)** during the MILAGRO campaign.

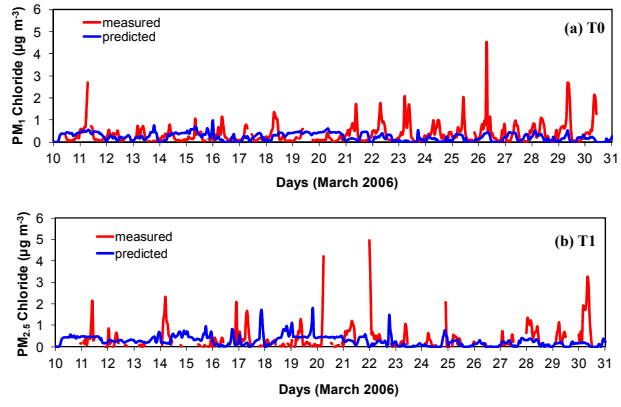

Fig. 8. Comparison of model hourly predictions against measurements for PM_1 chloride taken at T0 **(a)** and $PM_{2.5}$ chloride taken at T1 **(b)** during the MILAGRO campaign.

same hour is 3.3 ppb. This is probably due to the predicted OH levels as they are slightly underestimated during early morning even though they are reasonably reproduced by the model during the rest of the day (not shown). Therefore the formation of HNO_3 during the day from the reaction of NO_2

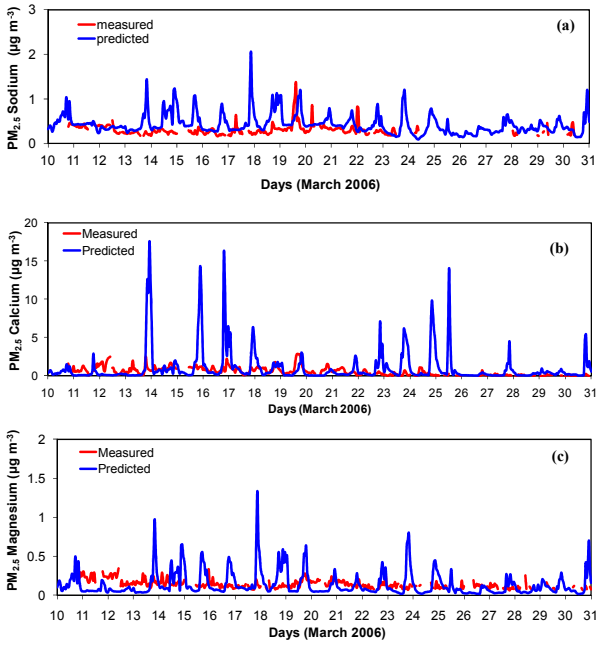

Fig. 9. Comparison of model hourly predictions against measurements for $PM_{2.5}$ **(a)** sodium, **(b)** calcium, **(c)** magnesium taken at T1 during the MILAGRO campaign.

with OH is limited in the model resulting eventually in an underprediction of the aerosol nitrate. Moreover, the total nitric acid produced in the center of Mexico City is transported to the north and is observed in T1 during the afternoon. Therefore, the underestimation of nitrate during the early morning at T0 is also observed 3 to 6 h later at T1 (Fig. 6d). Especially towards the last week of March 2006, the observed nitrate is much higher than the predicted one, so are HONO concentrations. Li et al. (2010) and Tsimpidi et al. (2010) have shown that the HONO production is quite important for the production of OH in the early morning atmosphere in the MCMA, suggesting that a more accurate description of HONO sources is needed. The inclusion of HONO emissions, used in this application, resulted in an average increase of 0.3 $\mu g\,m^{-3}$ in PM_1 nitrate concentration at T0 with a daily maximum of 0.9 $\mu g\,m^{-3}$ (at 11:00 LT). Moreover, the overestimation of dust components (see "dust components" subsection), especially calcium which originates from the Tolteca cement plant close to T1, affects the partitioning of nitric acid to the aerosol phase resulting in an over-prediction of nitrate at T1 early in the morning and late at night (Fig. 6d). Overall, the average predicted nitrate concentrations are 2.7 $\mu g\,m^{-3}$ and 3.2 $\mu g\,m^{-3}$ in T0 and T1 sites respectively while the observed averages were 3.5 $\mu g\,m^{-3}$ and 2.9 $\mu g\,m^{-3}$, respectively.

Ammonium: The ammonium predictions are quite sensitive to the ammonia emissions inventory, the predicted sulfate concentrations and the nitrate levels. The performance

of the model is respectable in both sites (Fig. 7) but it underpredicts ammonium concentrations during midday in T0 (Fig. 7b), due to the underprediction in total nitric acid. In T0 the average predicted concentration is 1.7 $\mu g\,m^{-3}$ while the observed average was 2.1 $\mu g\,m^{-3}$. Some of the difficulty in reproducing the hourly fluctuations of ammonium at T1 (Fig. 7c) is due to the sulfate predictions, as part of the ammonium in T1 exists in the aerosol phase in the form of ammonium sulfate. The predicted average $PM_{2.5}$ ammonium concentration in T1 is 1.4 $\mu g\,m^{-3}$ while the measured average is 1.5 $\mu g\,m^{-3}$.

Chloride: Both observations and predictions suggest that chloride concentrations remain at low levels (up to 0.5 $\mu g\,m^{-3}$) most of the time in both the T0 and T1 sites (Fig. 8). Nevertheless, there are some measured major spikes at T0 during the morning rush hours that the model is unable to reproduce (Fig. 8a). These spikes were observed mostly in the last week of the campaign. Given that the model uses the same HCl emissions for every week day, it should be investigated if these emissions were, for some reason, higher during this week. During this period there is a clear decrease in the number of fires due to higher precipitation and humidity (Fast et al., 2007). Surprisingly enough, measured chloride is higher during this low fire period, which indicates that despite the emission of chloride by fires (DeCarlo et al., 2008), urban sources and/or favorable partitioning conditions may be more important for this species in the MCMA. Comparisons of the predicted and measured diurnal profiles at T0 (Fig. 8b) suggest that the model underpredicts chloride. The average predicted concentration is 0.25 $\mu g\,m^{-3}$ while the observed average was 0.36 $\mu g\,m^{-3}$. Given that the AMS measures only non refractory chloride, the model underprediction of the ambient chloride concentration is probably greater. Aiken et al. (2009) suggest that approximately two thirds of the chloride is due to NH_4Cl or species of similarly high volatility, while the rest may be due to more refractory species such as $PbCl_2$ that are not simulated by the model. In T1, the predicted average $PM_{2.5}$ chloride concentration is 0.3 $\mu g\,m^{-3}$ while the measured average is 0.4 $\mu g\,m^{-3}$.

Dust components: Measurements of $PM_{2.5}$ sodium, calcium, and magnesium were only available at T1. PMCAMx-2008 shows on average a reasonable performance for these three dust components (Fig. 9). However, there is a tendency towards overprediction, especially for calcium (Fig. 9b), indicating a possible overestimation of the dust emissions that PMCAMx-2008 uses and probably errors in the contributions of the individual dust components or their size distribution. The predicted peaks at T1 for sodium, calcium, and magnesium are in the range of 1 $\mu g\,m^{-3}$, 10 $\mu g\,m^{-3}$, and 0.5 $\mu g\,m^{-3}$ respectively, while the measured peaks were in the range of 0.5 $\mu g\,m^{-3}$ for sodium, 3 $\mu g\,m^{-3}$ for calcium, and 0.3 $\mu g\,m^{-3}$ for magnesium. Despite the above weakness, the model captures relative well not only the daily average concentrations of the dust components, but also their average diurnal variation, as both the predicted and the measured profiles are flat with almost constant concentration. The daily average predicted concentrations of $PM_{2.5}$ sodium, calcium, and magnesium at T1 are 0.5 $\mu g\,m^{-3}$, 1.2 $\mu g\,m^{-3}$, and 0.15 $\mu g\,m^{-3}$ respectively, while the average measured concentrations of the same species were 0.3 $\mu g\,m^{-3}$, 0.6 $\mu g\,m^{-3}$ and 0.15 $\mu g\,m^{-3}$, respectively.

6 Sensitivity to inorganic aerosol dynamics

To estimate the effects of the hybrid aerosol thermodynamic approach on the formation of the semi-volatile inorganic aerosol components, the predictions of the model using the hybrid approach were compared against those using the equilibrium approach for the simulation of the partitioning of semivolatile inorganic PM components. The concentration difference in the fine and coarse mode between the predictions of these two modeling approaches for nitrate is shown in Fig. 10. Positive concentrations reflect increases due to the use of the hybrid approach.

Assuming bulk equilibrium between the gas and the aerosol phase results in an increase of the predicted PM_1 nitrate up to 2.5 $\mu g\,m^{-3}$ while, at the same time, the nitrate concentration on the coarse mode decreases by an equal amount. This significant change on the results is due to the fact that the bulk equilibrium algorithm distributes most of the total PM nitrate to the fine mode (approximately 90 %) that has most of the surface area. In the hybrid approach, the coarse fraction continues to absorb nitric acid vapors, even after the small particles achieve equilibrium, thus lowering the nitric acid gas-phase concentration. The smallest sections then lose mass as evaporation is required to maintain equilibrium with the gas phase. As a result the predicted coarse nitrate using the hybrid approach represents 55 % on average of the total PM nitrate. At T0 the average measured concentration of PM_1 nitrate is 3.5 $\mu g\,m^{-3}$. Using the hybrid approach for aerosol dynamics, the model underpredicts the average PM_1 nitrate concentration by 0.9 $\mu g\,m^{-3}$. Nevertheless, as discussed in section 5, this discrepancy is not caused by errors in size distribution or in the partitioning between the aerosol and the gas phases but in the underprediction of HONO formation and emissions. On the other hand, assuming bulk equilibrium between the gas and the aerosol phase, the model overpredicts the PM_1 nitrate concentration by 1.2 $\mu g\,m^{-3}$. This overprediction can be even larger if the model uses more accurate HONO emissions. At T1, where the impact of HONO emissions is not as important as at T0 (which is an urban site) and the dust concentration is higher than the urban center (which results in more nitrate in the coarse mode), the model, using the hybrid approach, agrees well with the observations for $PM_{2.5}$ nitrate (the mean bias is 0.1 $\mu g\,m^{-3}$). Using the bulk equilibrium approach though, results in an average overprediction of $PM_{2.5}$ nitrate by 1.2 $\mu g\,m^{-3}$. Therefore, the hybrid approach is considered

essential in order to accurately simulate the size distribution of the inorganic aerosols.

7 Sensitivity to emissions of inorganic aerosol precursors

In order to estimate the response of fine PM components to changes in anthropogenic emissions in Mexico City, three control strategies are examined separately, a 50 % reduction of SO_2, a 50 % reduction of NH_3, and a 50 % reduction of NO_x emissions. These should be viewed as sensitivity tests as they do not correspond to actual emission control strategies. The results of these simulations are compared to the results of the base case simulation to examine the effectiveness of these strategies in the reduction of PM_1 sulfate, nitrate, and ammonium concentrations.

The predicted changes in ground-level concentrations of the inorganic aerosols after a 50 % reduction of SO_2 emissions are shown in Fig. 11. Sulfate decreases by approximately 0.5 $\mu g\,m^{-3}$ (less than 5 %) in the Tula vicinity, where it has the highest concentration, while in the center of Mexico City the reduction of sulfate is approximately 0.3 $\mu g\,m^{-3}$ ($\sim$10 %). The highest reduction on the hourly average concentration is 8 $\mu g\,m^{-3}$ (25 %) in Tula. This extremely non linear response of sulfate concentration to the reduction of SO_2 emissions is in contrast with the findings of Tsimpidi et al. (2007) where sulfate concentration on the Eastern US varied linearly with SO_2 emissions, especially during the summer season. The main difference between the atmosphere of Mexico City and the eastern US is the concentration of SO_2 which in MCMA is predicted to be more than 10 times higher than in the eastern US. Therefore, the oxidant concentration in the area is not sufficient for the SO_2 oxidation to SO_4^{2-} and the production of the latter is more controlled by the availability of oxidants than of SO_2. Nitrate concentration increases up to 0.1 $\mu g\,m^{-3}$ (10 %) after the reduction of SO_2 emissions while the maximum increase on the hourly average concentration is 0.6 $\mu g\,m^{-3}$ (25 %). This increase is attributed to the increase of free ammonia, after the reduction of sulfate, which reacted with HNO_3 to form additional particulate nitrate. Ammonium concentration decreases by 0.1 $\mu g\,m^{-3}$ (5–10 %) in the center of Mexico City and the hourly maximum concentration decreases by 1 $\mu g\,m^{-3}$ (40 %). The reduction of ammonium in Tula is very small (0.02 $\mu g\,m^{-3}$ or 0.01 %) as ammonium sulfate represents a small fraction ($\sim$20 %) of total sulfate mass in the area. Overall, total PM_1 decreases by 1.3 % in Mexico City center and 1.1 % in Tula after a 50 % reduction of SO_2 emissions.

The predicted changes in ground-level concentrations of the inorganic aerosols after a 50 % reduction of NH_3 emissions are shown in Fig. 12. Sulfate concentration is not sensitive to changes on ammonia emissions as even in environments with low NH_3, sulfate still exists in the aerosol phase in the form of ammonium bisulfate or as H_2SO_4. In the center of Mexico City, after the 50 % reduction of NH_3 emissions, nitrate and ammonium decreases by 1 $\mu g\,m^{-3}$ (35 %) and 0.3 $\mu g\,m^{-3}$ (20 %) respectively. The highest reduction of ammonium concentration is predicted in Tula and is up to 1 $\mu g\,m^{-3}$ (35 %). The highest hourly average concentration of nitrate, located in Mexico City center, and ammonium, located in Tula, is reduced by 10 $\mu g\,m^{-3}$ (60 %) and 4 $\mu g\,m^{-3}$ (45 %) respectively. Overall, the predicted decrease of total PM_1 concentration after a 50 % reduction of NH_3 emissions is 4.4 % and 2 % in Mexico City center and Tula respectively.

The predicted changes in ground-level concentrations of the inorganic aerosols after a 50 % reduction of NO_x emissions are shown in Fig. 13. In the center of Mexico City, the decrease of NO_x emissions results in lower OH radical and ozone concentrations and consequently a decrease of sulfate concentration levels. In particular, sulfate decreases by up to 0.2 $\mu g\,m^{-3}$ (7 %) with an hourly maximum of 3.5 $\mu g\,m^{-3}$ (35 %). In Tula, a reduction of NO_x concentrations results in an increase of OH and O_3 concentrations and, as a result, sulfate concentration increases by 0.3 $\mu g\,m^{-3}$ (2 %) with an hourly maximum of 7 $\mu g\,m^{-3}$ (15 %). Nitrate decreases by 1 $\mu g\,m^{-3}$ (35 %), with an hourly maximum of 7.5 $\mu g\,m^{-3}$ (50 %), as NO_x is the main precursor of HNO_3 in the atmosphere. The simultaneously decrease of both nitrate and sulfate concentration levels in Mexico City resulted in a 0.3 $\mu g\,m^{-3}$ (20 %) decrease of ammonium concentration, with an hourly maximum of 2 $\mu g\,m^{-3}$ (45 %). When NO_x emissions are reduced in half, total PM_1 concentration decreases by 3.5 % and 0.1 % in Mexico City and Tula, respectively.

8 Conclusions

A detailed three-dimensional chemical transport model (PMCAMx-2008), which contains an advance thermodynamic description of the semivolatile inorganic components, is presented and applied during the MILAGRO-2006 campaign in the Mexico City Metropolitan Area. During this study, we evaluate the model against one of the best available datasets in a highly polluted urban area which includes one month of continuous measurements for the major inorganic aerosol components as well as filter-based measurements for the major mineral dust components in urban (T0) and suburban (T1) sites. This evaluation provides a valuable test of the current state-of-the-art in atmospheric inorganic aerosol modeling in a polluted megacity and is clearly a necessary step before the model can be used for the investigation of the efficiency of different emission control measures. Overall, PMCAMx-2008 was able to reproduce both the daily average concentrations and the diurnal variation of the major inorganic aerosol components.

Sulfate is regional in nature with clear influences from the large SO_2 sources in the industrial complex in Tula, while the

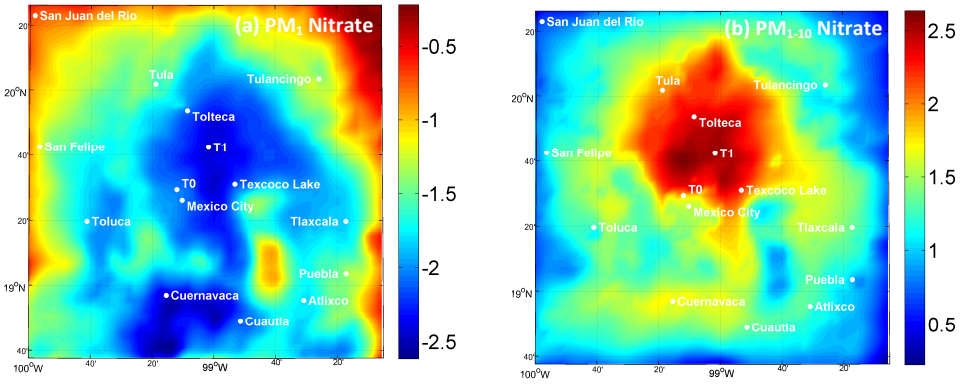

Fig. 10. Predicted change in ground-level concentrations ($\mu g\,m^{-3}$) of the **(a)** PM_1 nitrate and **(b)** PM_{1-10} nitrate after using the equilibrium approach for aerosol dynamics (instead of the hybrid approach used in the basecase simulations). A positive change corresponds to an increase due to the use of the hybrid approach.

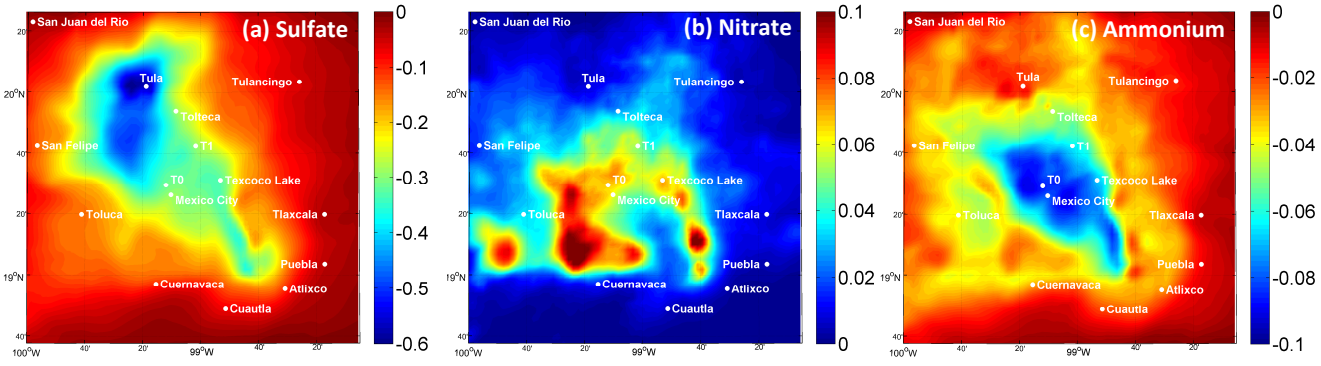

Fig. 11. Predicted change ($\mu g\,m^{-3}$) in ground-level concentrations of PM_1 **(a)** sulfate, **(b)** nitrate, and **(c)** ammonium after a 50 % reduction of SO_2 emissions. A negative change corresponds to a decrease.

urban area is not a major source of sulfate. Therefore, sulfate concentrations are high in Mexico City when the winds are northerly, while in periods where southerly winds are dominant, the concentrations of sulfate are lower. Nitrate is enhanced significantly in the urban area and immediate outflow (up to $3\,\mu g\,m^{-3}$), mostly produced from local photochemistry. It decreases with distance from the city, due to evaporation and deposition, remaining in low levels in the surroundings (lower than $1\,\mu g\,m^{-3}$). Nitrate underprediction during the early morning hours is attributed to the underestimation of OH levels by the model. An improvement of the simulation of HONO formation in the early morning can probably mitigate this weakness. Ammonium predictions are quite sensitive to the ammonia emissions inventory, the predicted sulfate concentrations and the nitrate levels. In particular, ammonium concentrations peak at the center of Mexico City and the Tula vicinity ($3\,\mu g\,m^{-3}$) existing mainly in the form of ammonium nitrate and ammonium sulfate, respectively.

The Texcoco dry Lake is a significant source of potassium (up to $1\,\mu g\,m^{-3}$), magnesium ($1\,\mu g\,m^{-3}$), sodium ($2\,\mu g\,m^{-3}$), and calcium ($3\,\mu g\,m^{-3}$) that influences the PM concentrations in the areas to the east and northeast of the city. Predicted calcium concentrations peak near Tolteca (up to $7\,\mu g\,m^{-3}$) as a result of emissions from the cement industries in the area. Its overerprediction though, indicates a possible overestimation of these emissions resulting also in an overprediction of nitrate during early in the morning and late at night at T1. In general, ISORROPIA-II assist the model in simulating the formation of the semivolatile inorganic PM as it includes interactions with the mineral dust components. The hybrid approach is also essential in order to accurately simulate the size distribution of the inorganic aerosols as the use of the bulk equilibrium approach results in unrealistically high PM_1 nitrate (over $5\,\mu g\,m^{-3}$) while, at the same time, the coarse nitrate concentration is seriously undepredicted.

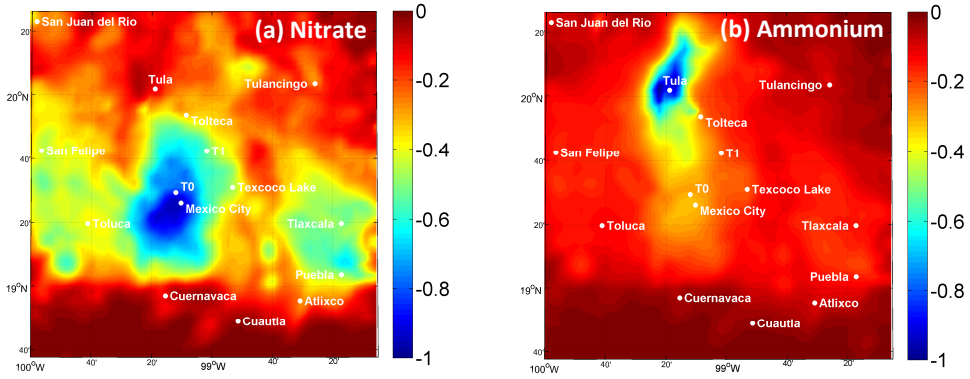

Fig. 12. Predicted change ($\mu g\,m^{-3}$) in ground-level concentrations of PM_1 **(a)** nitrate, and **(b)** ammonium after a 50 % reduction of NH_3 emissions. A negative change corresponds to a decrease.

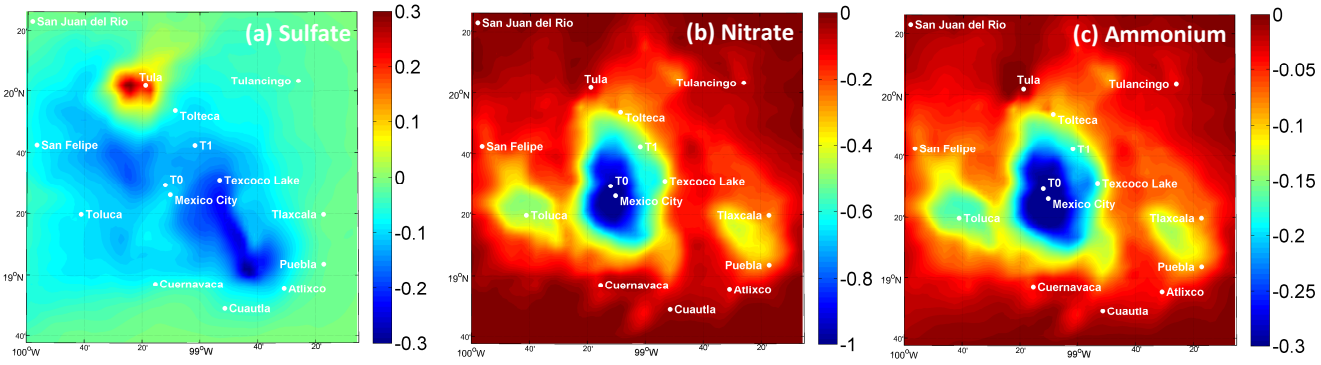

Fig. 13. Predicted change ($\mu g\,m^{-3}$) in ground-level concentrations of PM_1 **(a)** sulfate, **(b)** nitrate, and **(c)** ammonium after a 50 % reduction of NO_x emissions. A negative change corresponds to a decrease.

The sensitivity of fine PM components to changes in anthropogenic emissions in Mexico City was also examined. A 50 % reduction of SO_2 emissions leads to a decrease of average PM_1 sulfate and ammonium concentrations up to 0.5 $\mu g\,m^{-3}$ and 0.1 $\mu g\,m^{-3}$ respectively, and to an increase of PM_1 nitrate concentration up to 0.1 $\mu g\,m^{-3}$. A 50 % reduction of NH_3 emissions leads to a decrease of PM_1 nitrate and ammonium concentrations up to 1 $\mu g\,m^{-3}$ in Mexico City center and 1 $\mu g\,m^{-3}$ in Tula respectively. The ammonium concentration reduction in the center of Mexico City is up to 0.3 $\mu g\,m^{-3}$. Sulfate concentration is not sensitive to changes of ammonia emissions. A 50 % reduction of NO_x emissions leads to a decrease of PM_1 nitrate and ammonium concentrations up to 1 $\mu g\,m^{-3}$ and 0.3 $\mu g\,m^{-3}$ respectively. PM_1 sulfate concentration decreases by 0.2 $\mu g\,m^{-3}$ in Mexico City and increases by 0.3 $\mu g\,m^{-3}$ in Tula. These relatively small individual decreases reveal the challenge of reduce fine PM in Mexico City.

Overall, this study is part of a continuous effort to build a chemical transport model (PMCAMx) that can accurately describe the formation of both organic (Gaydos et al., 2007; Karydis et al., 2007; Lane et al., 2008; Shrivastava et al., 2008; Murphy and Pandis, 2009; Tsimpidi et al., 2010; Tsimpidi et al., 2011) and inorganic (Gaydos et al., 2007; Karydis et al., 2007; Karydis et al., 2010) aerosols in urban (Karydis et al., 2010; Tsimpidi et al., 2010; Tsimpidi et al., 2011) and regional (Gaydos et al., 2007; Karydis et al., 2007; Lane et al., 2008; Murphy and Pandis, 2009; Shrivastava et al., 2008) scales. PMCAMx has been tested successfully in different scales and environments (Murphy and Pandis, 2009; Tsimpidi et al., 2011; Fountoukis et al., 2011; current study). During this study, we have shown that the use of this or similar inorganic modeling frameworks is essential in order to accurately simulate the effects of mineral dust on the composition and the size distribution of the predicted inorganic aerosols.

Acknowledgements. This research was supported by the European Union and the 7th framework programme under the project MEGAPOLI (Grant agreement no.: 212520). LTM would like to acknowledge support from NSF (ATM-0528227).

Edited by: M. Gauss

References

Adhikary, B., Carmichael, G. R., Kulkarni, S., Wei, C., Tang, Y., D'Allura, A., Mena-Carrasco, M., Streets, D. G., Zhang, Q., Pierce, R. B., Al-Saadi, J. A., Emmons, L. K., Pfister, G. G., Avery, M. A., Barrick, J. D., Blake, D. R., Brune, W. H., Cohen, R. C., Dibb, J. E., Fried, A., Heikes, B. G., Huey, L. G., O'Sullivan, D. W., Sachse, G. W., Shetter, R. E., Singh, H. B., Campos, T. L., Cantrell, C. A., Flocke, F. M., Dunlea, E. J., Jimenez, J. L., Weinheimer, A. J., Crounse, J. D., Wennberg, P. O., Schauer, J. J., Stone, E. A., Jaffe, D. A., and Reidmiller, D. R.: A regional scale modeling analysis of aerosol and trace gas distributions over the eastern Pacific during the INTEX-B field campaign, Atmos. Chem. Phys., 10, 2091–2115, doi:10.5194/acp-10-2091-2010, 2010.

Aiken, A. C., Salcedo, D., Cubison, M. J., Huffman, J. A., DeCarlo, P. F., Ulbrich, I. M., Docherty, K. S., Sueper, D., Kimmel, J. R., Worsnop, D. R., Trimborn, A., Northway, M., Stone, E. A., Schauer, J. J., Volkamer, R. M., Fortner, E., de Foy, B., Wang, J., Laskin, A., Shutthanandan, V., Zheng, J., Zhang, R., Gaffney, J., Marley, N. A., Paredes-Miranda, G., Arnott, W. P., Molina, L. T., Sosa, G., and Jimenez, J. L.: Mexico City aerosol analysis during MILAGRO using high resolution aerosol mass spectrometry at the urban supersite (T0) Part 1: Fine particle composition and organic source apportionment, Atmos. Chem. Phys., 9, 6633–6653, doi:10.5194/acp-9-6633-2009, 2009.

Ansari, A. S. and Pandis, S. N.: Response of inorganic PM to precursor concentrations, Environ. Sci. Technol., 32, 2706–2714, 1998.

Ansari, A. S. and Pandis, S. N.: Prediction of multicomponent inorganic atmospheric aerosol behavior, Atmos. Environ., 33, 745–757, 1999a.

Ansari, A. S. and Pandis, S. N.: An analysis of four models predicting the partitioning of semivolatile inorganic aerosol components, Aerosol Sci. Technol., 31, 129–153, 1999b.

Ansari, A. S. and Pandis, S. N.: The effect of metastable equilibrium states on the partitioning of nitrate between the gas and aerosol phases, Atmos. Environ., 34, 157–168, 2000.

Apel, E. C., Emmons, L. K., Karl, T., Flocke, F., Hills, A. J., Madronich, S., Lee-Taylor, J., Fried, A., Weibring, P., Walega, J., Richter, D., Tie, X., Mauldin, L., Campos, T., Weinheimer, A., Knapp, D., Sive, B., Kleinman, L., Springston, S., Zaveri, R., Ortega, J., Voss, P., Blake, D., Baker, A., Warneke, C., Welsh-Bon, D., de Gouw, J., Zheng, J., Zhang, R., Rudolph, J., Junkermann, W., and Riemer, D. D.: Chemical evolution of volatile organic compounds in the outflow of the Mexico City Metropolitan area, Atmos. Chem. Phys., 10, 2353–2375, doi:10.5194/acp-10-2353-2010, 2010.

Arellano Jr., A. F., Raeder, K., Anderson, J. L., Hess, P. G., Emmons, L. K., Edwards, D. P., Pfister, G. G., Campos, T. L., and Sachse, G. W.: Evaluating model performance of an ensemble-based chemical data assimilation system during INTEX-B field mission, Atmos. Chem. Phys., 7, 5695–5710, doi:10.5194/acp-7-5695-2007, 2007.

Aumont, B., Chervier, F., and Laval, S.: Contribution of HONO sources to the $NO_x/HO_x/O^{-3}$ chemistry in the polluted boundary layer, Atmos. Environ., 37, 487–498, 2003.

Bassett, M. and Seinfeld, J. H.: Atmospheric equilibrium-model of sulfate and nitrate aerosols, Atmos. Environ., 17, 2237–2252, 1983.

Capaldo, K. P., Pilinis, C., and Pandis, S. N.: A computationally efficient hybrid approach for dynamic gas/aerosol transfer in air quality models, Atmos. Environ., 34, 3617–3627, 2000.

Carter, W. P. L.: Implementation of the SAPRC-99 chemical mechanism into the models-3 framework: http://citeseerx.ist.psu.edu/viewdoc/download?doi=10.1.1.25.293\&rep=rep1\&type=pdf, last access: 2 August 2011, 2000.

Chow, J. C. and Egami, R. T.: San Joaquin Valley 1995 integrated monitoring study: Documentation, evaluation, and descriptive data analysis of PM10, PM2.5, and precursor gas measurements. Technical Support Studies No. 4 and No. 8. Final Report prepared for the Technical Support Division, California Air Resources Board, Sacramento, CA by Desert Research Institute, Reno, NV, DRI Document No. 5460.1F1, 1997.

Clegg, S. L., Brimblecombe, P., and Wexler, A. S.: Thermodynamic model of the system H^+-NH_4^+-Na^+-SO_4^{2-}-NB_3^--Cl^--H_2O at 298.15 K, J. Phys. Chem. A, 102, 2155–2171, 1998a.

Clegg, S. L., Brimblecombe, P., and Wexler, A. S.: Thermodynamic model of the system H^+-NH_4^+-SO_4^{2-}-NO_3^--H_2O at tropospheric temperatures, J. Phys. Chem. A, 102, 2137–2154, 1998b.

Dassios, K. G. and Pandis, S. N.: The mass accommodation coefficient of ammonium nitrate aerosol, Atmos. Environ., 33, 2993–3003, doi:10.1016/s1352-2310(99)00079-5, 1999.

DeCarlo, P. F., Kimmel, J. R., Trimborn, A., Northway, M. J., Jayne, J. T., Aiken, A. C., Gonin, M., Fuhrer, K., Horvath, T., Docherty, K. S., Worsnop, D. R., and Jimenez, J. L.: Field-deployable, high-resolution, time-of-flight aerosol mass spectrometer, Anal. Chem., 78, 8281–8289, doi:10.1021/ac061249n, 2006.

DeCarlo, P. F., Dunlea, E. J., Kimmel, J. R., Aiken, A. C., Sueper, D., Crounse, J., Wennberg, P. O., Emmons, L., Shinozuka, Y., Clarke, A., Zhou, J., Tomlinson, J., Collins, D. R., Knapp, D., Weinheimer, A. J., Montzka, D. D., Campos, T., and Jimenez, J. L.: Fast airborne aerosol size and chemistry measurements above Mexico City and Central Mexico during the MILAGRO campaign, Atmos. Chem. Phys., 8, 4027–4048, doi:10.5194/acp-8-4027-2008, 2008.

Draxler, R. R., Gillette, D. A., Kirkpatrick, J. S., and Heller, J.: Estimating PM_{10} air concentrations from dust storms in Iraq, Kuwait and Saudi Arabia, Atmos. Environ., 35, 4315–4330, 2001.

Environ: User's guide to the comprehensive air quality model with extensions (CAMx). Version 4.02. Report prepared by ENVIRON International Corporation, Novato, CA. , 2003.

Fahey, K. M. and Pandis, S. N.: Optimizing model performance: variable size resolution in cloud chemistry modeling, Atmos. Environ., 35, 4471–4478, 2001.

Fast, J. D., de Foy, B., Acevedo Rosas, F., Caetano, E., Carmichael, G., Emmons, L., McKenna, D., Mena, M., Skamarock, W., Tie, X., Coulter, R. L., Barnard, J. C., Wiedinmyer, C., and Madronich, S.: A meteorological overview of the MILAGRO field campaigns, Atmos. Chem. Phys., 7, 2233–2257, doi:10.5194/acp-7-2233-2007, 2007.

Fast, J., Aiken, A. C., Allan, J., Alexander, L., Campos, T., Canagaratna, M. R., Chapman, E., DeCarlo, P. F., de Foy, B., Gaffney, J., de Gouw, J., Doran, J. C., Emmons, L., Hodzic, A., Herndon, S. C., Huey, G., Jayne, J. T., Jimenez, J. L., Kleinman, L., Kuster, W., Marley, N., Russell, L., Ochoa, C., Onasch, T. B., Pekour, M., Song, C., Ulbrich, I. M., Warneke, C., Welsh-Bon, D., Wiedinmyer, C., Worsnop, D. R., Yu, X.-Y., and Zaveri, R.: Evaluating simulated primary anthropogenic and biomass

burning organic aerosols during MILAGRO: implications for assessing treatments of secondary organic aerosols, Atmos. Chem. Phys., 9, 6191–6215, doi:10.5194/acp-9-6191-2009, 2009.

Finlayson-Pitts, B. J. and Pitts, J. N.: Chemistry of the Upper and Lower Atmosphere, Academic Press, San Diego, 2000.

Fountoukis, C. and Nenes, A.: ISORROPIA II: a computationally efficient thermodynamic equilibrium model for K^+-Ca^{2+}-Mg^{2+}-NH_4^+-Na^+-SO_4^{2-}-NO_3^--Cl^--H_2O aerosols, Atmos. Chem. Phys., 7, 4639–4659, doi:10.5194/acp-7-4639-2007, 2007.

Fountoukis, C., Nenes, A., Sullivan, A., Weber, R., Van Reken, T., Fischer, M., Matas, E., Moya, M., Farmer, D., and Cohen, R. C.: Thermodynamic characterization of Mexico City aerosol during MILAGRO 2006, Atmos. Chem. Phys., 9, 2141–2156, doi:10.5194/acp-9-2141-2009, 2009.

Fountoukis, C., Racherla, P. N., Denier van der Gon, H. A. C., Polymeneas, P., Charalampidis, P. E., Pilinis, C., Wiedensohler, A., Dall'Osto, M., O'Dowd, C., and Pandis, S. N.: Evaluation of a three-dimensional chemical transport model (PMCAMx) in the European domain during the EUCAARI May 2008 campaign, Atmos. Chem. Phys., 11, 10331–10347, doi:10.5194/acp-11-10331-2011, 2011.

Gaydos, T. M., Pinder, R., Koo, B., Fahey, K. M., Yarwood, G., and Pandis, S. N.: Development and application of a three-dimensional aerosol chemical transport model, PMCAMx, Atmos. Environ., 41, 2594–2611, doi:10.1016/j.atmosenv.2006.11.034, 2007.

Gaydos, T. M., Koo, B., Pandis, S. N., and Chock, D. P.: Development and application of an efficient moving sectional approach for the solution of the atmospheric aerosol condensation/evaporation equations, Atmos. Environ., 37, 3303–3316, doi:10.1016/s1352-2310(03)00267-x, 2003.

Hildemann, L. M., Russell, A. G., and Cass, G. R.: Ammonia and nitric-acid concentrations in equilibrium with atmospheric aerosols – experiment vs. theory, Atmos. Environ., 18, 1737-1750, 1984.

Hodzic, A., Jimenez, J. L., Madronich, S., Aiken, A. C., Bessagnet, B., Curci, G., Fast, J., Lamarque, J.-F., Onasch, T. B., Roux, G., Schauer, J. J., Stone, E. A., and Ulbrich, I. M.: Modeling organic aerosols during MILAGRO: importance of biogenic secondary organic aerosols, Atmos. Chem. Phys., 9, 6949–6981, doi:10.5194/acp-9-6949-2009, 2009.

Hodzic, A., Jimenez, J. L., Madronich, S., Canagaratna, M. R., DeCarlo, P. F., Kleinman, L., and Fast, J.: Modeling organic aerosols in a megacity: potential contribution of semi-volatile and intermediate volatility primary organic compounds to secondary organic aerosol formation, Atmos. Chem. Phys., 10, 5491–5514, doi:10.5194/acp-10-5491-2010, 2010.

Jacobson, M. Z.: Development and application of a new air pollution modeling system .2. Aerosol module structure and design, Atmos. Environ., 31, 131–144, 1997a.

Jacobson, M. Z., Tabazadeh, A., and Turco, R. P.: Simulating equilibrium within aerosols and nonequilibrium between gases and aerosols, J. Geophys. Res.-Atmos., 101, 9079–9091, 1996.

Jacobson, M. Z.: Numerical techniques to solve condensational and dissolutional growth equations when growth is coupled to reversible reactions, Aerosol Sci. Technol., 27, 491–498, 1997b.

Jacobson, M. Z.: Studying the effects of calcium and magnesium on size-distributed nitrate and ammonium with EQUISOLV II, Atmos. Environ., 33, 3635–3649, 1999.

Karydis, V. A., Tsimpidi, A. P., and Pandis, S. N.: Evaluation of a three-dimensional chemical transport model (PMCAMx) in the eastern United States for all four seasons, J. Geophys. Res.-Atmos., 112, D14211, doi:10.1029/2006jd007890, 2007.

Karydis, V. A., Tsimpidi, A. P., Fountoukis, C., Nenes, A., Zavala, M., Lei, W. F., Molina, L. T., and Pandis, S. N.: Simulating the fine and coarse inorganic particulate matter concentrations in a polluted megacity, Atmos. Environ., 44, 608–620, doi:10.1016/j.atmosenv.2009.11.023, 2010.

Kim, Y. P. and Seinfeld, J. H.: Atmospheric gas-aerosol equilibrium .3. Thermodynamics of crustal elements Ca^{2+}, K^+, and Mg^{2+}, Aerosol Sci. Technol., 22, 93–110, 1995.

Kim, Y. P., Seinfeld, J. H., and Saxena, P.: Atmospheric gas-aerosol equilibrium 2. Analysis of common approximations and activity-coefficient calculation methods, Aerosol Sci. Technol., 19, 182–198, 1993a.

Kim, Y. P., Seinfeld, J. H., and Saxena, P.: Atmospheric gas aerosol equilibrium .1. Thermodynamic model, Aerosol Sci. Technol., 19, 157–181, 1993b.

Koo, B. Y., Ansari, A. S., and Pandis, S. N.: Integrated approaches to modeling the organic and inorganic atmospheric aerosol components, Atmos. Environ., 37, 4757–4768, doi:10.1016/j.atmosenv.2003.08.016, 2003.

Kumar, N., Lurmann, F. W., Pandis, S. N., and Ansari, A. S.: Final Report: analysis of atmospheric chemistry during 1995 integrated monitoring study. Final Report Prepared for the California Air Resources Board, Sacramento, CA by Sonoma Technology Inc., Santa Rosa, CA.STI-997214-1791-DFR, 1998.

Lane, T. E., Donahue, N. M., and Pandis, S. N.: Simulating secondary organic aerosol formation using the volatility basis-set approach in a chemical transport model, Atmos. Environ., 42, 7439–7451, doi:10.1016/j.atmosenv.2008.06.026, 2008.

Lawson, D. R.: The southern california air-quality study, J. Air Waste Manage. Assoc., 40, 156–165, 1990.

Li, G., Lei, W., Zavala, M., Volkamer, R., Dusanter, S., Stevens, P., and Molina, L. T.: Impacts of HONO sources on the photochemistry in Mexico City during the MCMA-2006/MILAGO Campaign, Atmos. Chem. Phys., 10, 6551–6567, doi:10.5194/acp-10-6551-2010, 2010.

Li, G., Zavala, M., Lei, W., Tsimpidi, A. P., Karydis, V. A., Pandis, S. N., Canagaratna, M. R., and Molina, L. T.: Simulations of organic aerosol concentrations in Mexico City using the WRF-CHEM model during the MCMA-2006/MILAGRO campaign, Atmos. Chem. Phys., 11, 3789–3809, doi:10.5194/acp-11-3789-2011, 2011a.

Li, G., Bei, N., Tie, X., and Molina, L. T.: Aerosol effects on the photochemistry in Mexico City during MCMA-2006/MILAGRO campaign, Atmos. Chem. Phys., 11, 5169–5182, doi:10.5194/acp-11-5169-2011, 2011b.

Lurmann, F. W., Wexler, A. S., Pandis, S. N., Musarra, S., Kumar, N., and Seinfeld, J. H.: Modelling urban and regional aerosols .2. Application to California's South Coast Air Basin, Atmos. Environ., 31, 2695–2715, 1997.

Meng, Z. Y. and Seinfeld, J. H.: Time scales to achieve atmospheric gas-aerosol equilibrium for volatile species, Atmos. Environ., 30, 2889–2900, doi:10.1016/1352-2310(95)00493-9, 1996.

Meng, Z. Y., Seinfeld, J. H., Saxena, P., and Kim, Y. P.: Atmospheric gas-aerosol equilibrium .4. Thermodynamics of

carbonates, Aerosol Sci. Technol., 23, 131–154, 1995.

Meng, Z. Y., Dabdub, D., and Seinfeld, J. H.: Size-resolved and chemically resolved model of atmospheric aerosol dynamics, J. Geophys. Res.-Atmos., 103, 3419–3435, 1998.

Michalakes, J., Dudhia, J., Gill, D., Henderson, T., Klemp, J., Skamarock, W., and Wang, W.: The weather research and forecast model: Software architecture and performance, Use of High Performance Computing in Meteorology, edited by: Zwieflhofer, W. and Mozdzynski, G., World Scientific Publ. Co Pte Ltd, Singapore, 156–168, 2005.

Molina, L. T. and Molina, M. J.: Air Quality in the Mexico Megacity: An Integrated Assessment, Kluwer Academic Publishers, Dordrecht, The Netherlands, 2002.

Molina, L. T., Madronich, S., Gaffney, J. S., Apel, E., de Foy, B., Fast, J., Ferrare, R., Herndon, S., Jimenez, J. L., Lamb, B., Osornio-Vargas, A. R., Russell, P., Schauer, J. J., Stevens, P. S., Volkamer, R., and Zavala, M.: An overview of the MILAGRO 2006 Campaign: Mexico City emissions and their transport and transformation, Atmos. Chem. Phys., 10, 8697–8760, doi:10.5194/acp-10-8697-2010, 2010.

Moya, M., Madronich, S., Retama, A., Weber, R., Baumann, K., Nenes, A., Castillejos, M., and de Leon, C. P.: Identification of chemistry-dependent artifacts on gravimetric PM fine readings at the T1 site during the MILAGRO field campaign, Atmos. Environ., 45, 244–252, doi:10.1016/j.atmosenv.2010.08.059, 2011.

Murphy, B. N. and Pandis, S. N.: Simulating the Formation of Semivolatile Primary and Secondary Organic Aerosol in a Regional Chemical Transport Model, Environ. Sci. Technol., 43, 4722–4728, doi:10.1021/es803168a, 2009.

Nenes, A., Pandis, S. N., and Pilinis, C.: ISORROPIA: A new thermodynamic equilibrium model for multiphase multicomponent inorganic aerosols, Aquat. Geochem., 4, 123–152, 1998.

Nenes, A., Pandis, S. N., and Pilinis, C.: Continued development and testing of a new thermodynamic aerosol module for urban and regional air quality models, Atmos. Environ., 33, 1553–1560, 1999.

Nguyen, M. T., Jamka, A. J., Cazar, R. A., and Tao, F. M.: Structure and stability of the nitric acid ammonia complex in the gas phase and in water, J. Chem. Phys., 106, 8710–8717, doi:10.1063/1.473925, 1997.

Orsini, D. A., Ma, Y. L., Sullivan, A., Sierau, B., Baumann, K., and Weber, R. J.: Refinements to the particle-into-liquid sampler (PILS) for ground and airborne measurements of water soluble aerosol composition, Atmos. Environ., 37, 1243–1259, doi:10.1016/S1352-2310(02)01015-4, 2003.

Pandis, S. N., Wexler, A. S., and Seinfeld, J. H.: Secondary organic aerosol formation and transport 2. Predicting the ambient secondary organic aerosol-size distribution, Atmos. Environ. A-Gen., 27, 2403–2416, 1993.

Pilinis, C. and Seinfeld, J. H.: Continued development of a general equilibrium-model for inorganic multicomponent atmospheric aerosols, Atmos. Environ., 21, 2453–2466, 1987.

Pilinis, C. and Seinfeld, J. H.: Development and evaluation of an eulerian photochemical gas aerosol model, Atmos. Environ., 22, 1985–2001, 1988.

Pilinis, C., Capaldo, K. P., Nenes, A., and Pandis, S. N.: MADM – A new multicomponent aerosol dynamics model, Aerosol Sci. Technol., 32, 482–502, doi:10.1080/027868200303597, 2000.

Racherla, P. N. and Adams, P. J.: Sensitivity of global tropospheric ozone and fine particulate matter concentrations to climate change, J. Geophys. Res.-Atmos., 111, D24103, doi:10.1029/2005jd006939, 2006.

Russell, A. G., McCue, K. F., and Cass, G. R.: Mathematical-modeling of the formation of nitrogen-containing air-pollutants 1. Evaluation of an eulerian photochemical model, Environ. Sci. Technol., 22, 263–270, 1988.

Saxena, P., Hudischewskyj, A. B., Seigneur, C., and Seinfeld, J. H.: A comparative-study of equilibrium approaches to the chemical characterization of secondary aerosols, Atmos. Environ., 20, 1471–1483, 1986.

Seinfeld, J. H. and Pandis, S. N.: Atmospheric Chemistry and Physics: From Air Pollution to Climate Change, 2nd edn., John Wiley & Sons, Inc., Hoboken, New Jersey, USA, 2006.

Shinozuka, Y., Clarke, A. D., DeCarlo, P. F., Jimenez, J. L., Dunlea, E. J., Roberts, G. C., Tomlinson, J. M., Collins, D. R., Howell, S. G., Kapustin, V. N., McNaughton, C. S., and Zhou, J.: Aerosol optical properties relevant to regional remote sensing of CCN activity and links to their organic mass fraction: airborne observations over Central Mexico and the US West Coast during MILAGRO/INTEX-B, Atmos. Chem. Phys., 9, 6727–6742, doi:10.5194/acp-9-6727-2009, 2009.

Shrivastava, M., Fast, J., Easter, R., Gustafson, W. I., Zaveri, R. A., Jimenez, J. L., Saide, P., and Hodzic, A.: Modeling organic aerosols in a megacity: comparison of simple and complex representations of the volatility basis set approach, Atmos. Chem. Phys., 11, 6639–6662, doi:10.5194/acp-11-6639-2011, 2011.

Shrivastava, M. K., Lane, T. E., Donahue, N. M., Pandis, S. N., and Robinson, A. L.: Effects of gas particle partitioning and aging of primary emissions on urban and regional organic aerosol concentrations, J. Geophys. Res.-Atmos., 113, D18301, doi:10.1029/2007jd009735, 2008.

Singh, H. B., Brune, W. H., Crawford, J. H., Flocke, F., and Jacob, D. J.: Chemistry and transport of pollution over the Gulf of Mexico and the Pacific: spring 2006 INTEX-B campaign overview and first results, Atmos. Chem. Phys., 9, 2301–2318, doi:10.5194/acp-9-2301-2009, 2009.

Song, J., Lei, W., Bei, N., Zavala, M., de Foy, B., Volkamer, R., Cardenas, B., Zheng, J., Zhang, R., and Molina, L. T.: Ozone response to emission changes: a modeling study during the MCMA-2006/MILAGRO Campaign, Atmos. Chem. Phys., 10, 3827–3846, doi:10.5194/acp-10-3827-2010, 2010.

Stokes, R. H. and Robinson, R. A.: Interactions in aqueous nonelectrolyte solutions. I. Solute-solvent equilibria, J. Phys. Chem., 70, 2126–2131, doi:10.1021/j100879a010, 1966.

Tanner, R. L.: An ambient experimental-study of phase-equilibrium in the atmospheric system-aerosol H^+, NH_4^+, SO_4^{2-}, NO_3^-, NH_3(g), HNO_3(g), Atmos. Environ., 16, 2935–2942, 1982.

Tie, X., Madronich, S., Li, G., Ying, Z., Weinheimer, A., Apel, E., and Campos, T.: Simulation of Mexico City plumes during the MIRAGE-Mex field campaign using the WRF-Chem model, Atmos. Chem. Phys., 9, 4621–4638, doi:10.5194/acp-9-4621-2009, 2009.

Tsimpidi, A. P., Karydis, V. A., and Pandis, S. N.: Response of inorganic fine particulate matter to emission changes of sulfur dioxide and ammonia: The eastern United States as a case study, J. Air Waste Manage. Assoc., 57, 1489–1498, doi:10.3155/1047-3289.57.12.1489, 2007.

Tsimpidi, A. P., Karydis, V. A., Zavala, M., Lei, W., Molina, L.,

Ulbrich, I. M., Jimenez, J. L., and Pandis, S. N.: Evaluation of the volatility basis-set approach for the simulation of organic aerosol formation in the Mexico City metropolitan area, Atmos. Chem. Phys., 10, 525–546, doi:10.5194/acp-10-525-2010, 2010.

Tsimpidi, A. P., Karydis, V. A., Zavala, M., Lei, W., Bei, N., Molina, L., and Pandis, S. N.: Sources and production of organic aerosol in Mexico City: insights from the combination of a chemical transport model (PMCAMx-2008) and measurements during MILAGRO, Atmos. Chem. Phys., 11, 5153–5168, doi:10.5194/acp-11-5153-2011, 2011.

Vega, E., Mugica, V., Reyes, E., Sanchez, G., Chow, J. C., and Watson, J. G.: Chemical composition of fugitive dust emitters in Mexico City, Atmos. Environ., 35, 4033–4039, 2001.

Voss, P. B., Zaveri, R. A., Flocke, F. M., Mao, H., Hartley, T. P., DeAmicis, P., Deonandan, I., Contreras-Jimenez, G., Martinez-Antonio, O., Estrada, M. F., Greenberg, D., Campos, T. L., Weinheimer, A. J., Knapp, D. J., Montzka, D. D., Crounse, J. D., Wennberg, P. O., Apel, E., Madronich, S., and de Foy, B.: Long-range pollution transport during the MILAGRO-2006 campaign: a case study of a major Mexico City outflow event using free-floating altitude-controlled balloons, Atmos. Chem. Phys., 10, 7137–7159, doi:10.5194/acp-10-7137-2010, 2010.

Watson, J. G., Chow, J. C., Lurmann, F. W., and Musarra, S. P.: Ammonium-nitrate, nitric-acid, and ammonia equilibrium in wintertime Phoenix, Arizona, J. Air Waste Manage. Assoc., 44, 405–412, 1994.

Wexler, A. S., and Seinfeld, J. H.: 2nd-generation inorganic aerosol model, Atmos. Environ. A-Gen., 25, 2731–2748, 1991.

Ying, Z. M., Tie, X. X., Madronich, S., Li, G. H., and Massie, S.: Simulation of regional dust and its effect on photochemistry in the Mexico City area during MILAGRO experiment, Atmos. Environ., 45, 2549–2558, doi:10.1016/j.atmosenv.2011.02.018, 2011.

Zaveri, R. A., Easter, R. C., Fast, J. D., and Peters, L. K.: Model for Simulating Aerosol Interactions and Chemistry (MOSAIC), J. Geophys. Res.-Atmos., 113, D13204, doi:10.1029/2007jd008782, 2008.

Zhang, K. M. and Wexler, A. S.: Modeling urban and regional aerosols – Development of the UCD Aerosol Module and implementation in CMAQ model, Atmos. Environ., 42, 3166–3178, doi:10.1016/j.atmosenv.2007.12.052, 2008.

Zhang, Y., Seigneur, C., Seinfeld, J. H., Jacobson, M., Clegg, S. L., and Binkowski, F. S.: A comparative review of inorganic aerosol thermodynamic equilibrium modules: similarities, differences, and their likely causes, Atmos. Environ., 34, 117–137, 2000.

Zhang, J., Chameides, W. L., Weber, R., Cass, G., Orsini, D., Edgerton, E., Jongejan, P., and Slanina, J.: An evaluation of the thermodynamic equilibrium assumption for fine particulate composition: Nitrate and ammonium during the 1999 Atlanta Supersite Experiment, J. Geophys. Res.-Atmos., 108, 8414, doi:10.1029/2001jd001592, 2002.

Zhang, Y., Dubey, M. K., Olsen, S. C., Zheng, J., and Zhang, R.: Comparisons of WRF/Chem simulations in Mexico City with ground-based RAMA measurements during the 2006-MILAGRO, Atmos. Chem. Phys., 9, 3777–3798, doi:10.5194/acp-9-3777-2009, 2009.

Zheng, J., Zhang, R., Fortner, E. C., Volkamer, R. M., Molina, L., Aiken, A. C., Jimenez, J. L., Gaeggeler, K., Dommen, J., Dusanter, S., Stevens, P. S., and Tie, X.: Measurements of HNO_3 and N_2O_5 using ion drift-chemical ionization mass spectrometry during the MILAGRO/MCMA-2006 campaign, Atmos. Chem. Phys., 8, 6823–6838, doi:10.5194/acp-8-6823-2008, 2008.